

**Catalysis of Carbon Dioxide and Oxetanes to Produce
Aliphatic Polycarbonates**

Journal:	<i>Green Chemistry</i>
Manuscript ID	GC-CRV-09-2020-003219.R2
Article Type:	Critical Review
Date Submitted by the Author:	26-Oct-2020
Complete List of Authors:	Bhat, Gulzar; Texas A&M University, Chemistry; Indian Institute of Technology Bombay, Chemistry Luo, Ming; Changshu Institute of Technology, School of Materials Engineering; Darensbourg, Donald; Texas A&M University,

Catalysis of Carbon Dioxide and Oxetanes to Produce Aliphatic Polycarbonates

By

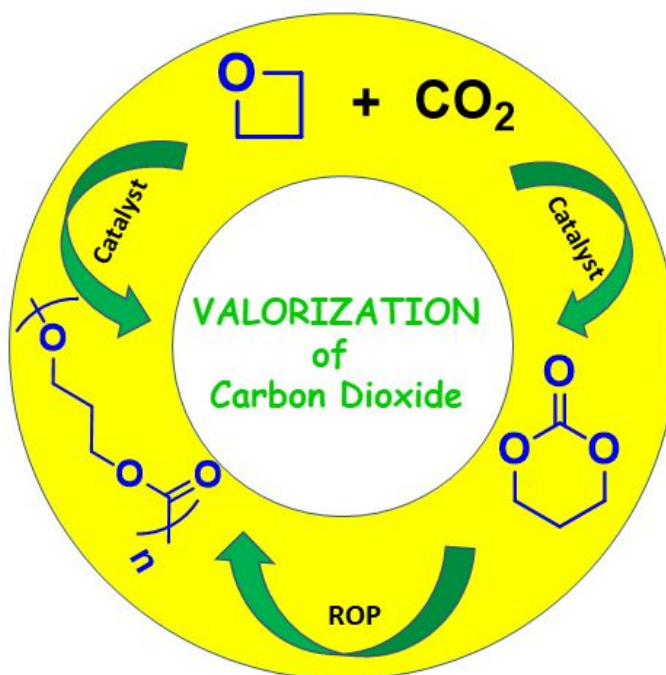
Gulzar A. Bhat¹, Ming Luo^{2*}, and Donald J. Darensbourg^{1*}

¹ Department of Chemistry, Texas A&M University, College Station, Texas 77843, United States

² School of Materials Engineering, Changshu Institute of Technology, Changshu, Jiangsu 215500, China

Synopsis

This review summarizes the literature for the coupling of CO₂ and oxetanes utilizing a broad range of metal and metal-free catalysts for the production of copolymers either directly or *via* ring-opening polymerization of preformed cyclic carbonates



Abstract

Although the coupling of CO₂ and a variety of epoxides is a well-developed area of study which has been extensively reviewed in the open literature, analogous processes involving CO₂ and oxetanes are much less investigated. In this review, we will summarize the reports which utilize a broad range of metal and metal-free catalysts for the coupling of CO₂ and oxetanes to afford copolymers, either directly or *via* the ring-opening polymerization of preformed six-membered cyclic carbonates. Comparative mechanistic aspects of these two CO₂/cyclic ethers coupling processes are presented along with the related processes involving sulfur analogs of carbon dioxide.

Keywords: *Carbon Dioxide, Oxetane, Copolymerization, Trimethylene Oxide, Ring-Opening Polymerization.*

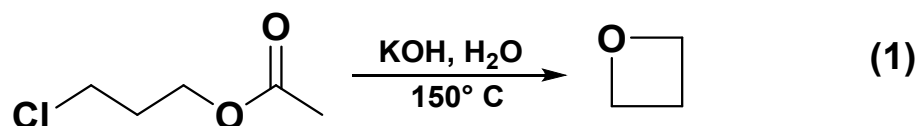
Introduction

Over the last 75 years our lives have been greatly improved in numerous ways by the development of a wide variety of plastics. Most of these polymeric materials are derived from petroleum-based chemicals and generally degrade over long periods of time.¹ For example, two of the most commonly used plastics, polyethylene and polypropylene, have lifespans of approximately 500 years in landfills. The stress to the environment of disposing of many of these materials has become a major worldwide concern.² Hence, there is much emphasis on developing biodegradable/degradable useful polymers, preferentially from renewable resources. Presently, one of the most prominent biodegradable polymers derived from renewable resources is polylactic acid (PLA).³

CO₂-based polymers are receiving much current attention for their use as sustainable materials, because of their biodegradability and varied properties. The most preeminent CO₂-derived copolymers are polycarbonates stemming from the catalytic coupling of carbon dioxide and oxiranes (epoxides).⁴⁻²¹ Relevant to the success of this process, which must overcome the thermodynamic stability of the CO₂ molecule, is the high ring-strain energies of the epoxide comonomers. Four-membered cyclic ethers, *oxetanes*, have similar high ring-strain energies. In 1965, Pell and Pilcher measured heat of combustion data for the three-, four-, and five-membered cyclic ethers in the gas phase at 25 °C and atmospheric pressure by flame calorimetry.²² Upon applying Allen's bond energy scheme they calculated the ring-strain energies of these cyclic ethers to be 114.1, 106.7, and 23.56 kJ/mol, respectively.²³ Hence, these ring-strain energies for cyclic ethers are very similar to those of the corresponding cycloalkanes, and considerably more energetic than cyclic sulfides. Since the copolymerization of CO₂ and oxiranes relies on the release of ring-strain from the oxirane monomer as the driving force for the polymerization, it would be anticipated that a similar process would be favorable for CO₂ and oxetanes. On the other hand, the related process involving tetrahydrofuran would be highly reversible.

However, the copolymerization of oxetanes and CO₂ are much less studied than the equivalent process with oxiranes. This is probably because fewer oxetanes are commercially available in bulk, and those that are, are generally quite expensive for use in polymer synthesis. For example, 10g of trimethylene oxide sells for \$212 from Sigma-Aldrich.²⁴ Nevertheless, the

unsubstituted oxetane, trimethylene oxide, can be prepared from potassium hydroxide and 3-chloropropyl acetate in 40% yield (eqn. 1).²⁵⁻²⁷ An improved, greener synthesis of oxetane has more recently been reported using an ionic liquid-based reagent as a replacement for Mitsunobu reagent.²⁸ In this method, oxetane has been produced in an 86 % yield from 1,3-propanediol *via* an intramolecular Mitsunobu reaction. Importantly, the recovered ionic liquid was shown to be recyclable for at least ten cycle with little loss in catalytic activity. It is noteworthy that 1,3-propanediol can be obtained on a large scale from glycerol, a major byproduct of biodiesel, or directly from glucose, by fermentation processes, thereby providing a more sustainable chemistry for the production of the important biodegradable polymer, poly(trimethylene carbonate).²⁹⁻³¹ Presently, there is much interest being directed at the development synthetic methodologies for the preparation of a wide range of oxetane derivatives for applications in medicinal chemistries.³² Hence, there are numerous significant studies detailing the copolymerization of CO₂ and oxetanes which we will summarize in this review. The preponderance of these processes are catalyzed *via*



a wide range of metal coordination complexes, however, recent investigations of organocatalysts for this process have been reported. It is noteworthy that the alternative product from the coupling of CO₂ and oxetanes, cyclic six-membered carbonates, are prone to ring-opening polymerization to provide mostly linear polycarbonates. By way of contrast, generally five-membered cyclic carbonates are thermodynamically more stable than their polymeric linear counterparts.

Mechanistic Aspects Common to CO₂/Oxetane and CO₂/Epoxide Copolymerization Reactions

The coordination-activation insertion mechanism for the copolymerization of CO₂/oxetane and CO₂/epoxide in the presence of metal-based catalysts share many intermediates in common, however, the reactivity of these can be saliently different (**Figure 1**). At the initiation of the two pathways there is a significant discrepancy, i.e., the monomer (cyclic ether) binding and ring-opening steps. In the case of epoxides, this process is very fast at ambient temperature in the attendance of good added nucleophiles, such as azide or chloride, with only the ring-opened metal-

alkoxide being observed.³³ By way of contrast, the metal-oxetane intermediate has been observed and characterized by X-ray crystallography (*vide infra*).³⁴ This is indicative of a greatly retarded rate of ring-opening of the oxetane monomer compared to that of the oxirane analogue. Furthermore, the metal binding ability of oxetane monomers are expected to be significantly better than that of epoxides, as noted by pK_b measurements. For example, the pK_b of trimethylene oxide (TMO) is over two-orders of magnitude lower than propylene oxide.³⁵ This is manifested in the observation that the terpolymerization of TMO (1,3-propylene oxide), propylene oxide (1,2-propylene oxide), and CO_2 does not occur under reaction conditions where TMO and CO_2 are unreactive, but propylene oxide and CO_2 readily undergoes polymerization to poly(propylene carbonate).³⁵ That is, TMO inhibits activation of the PO monomer because of TMO's superior metal binding ability.

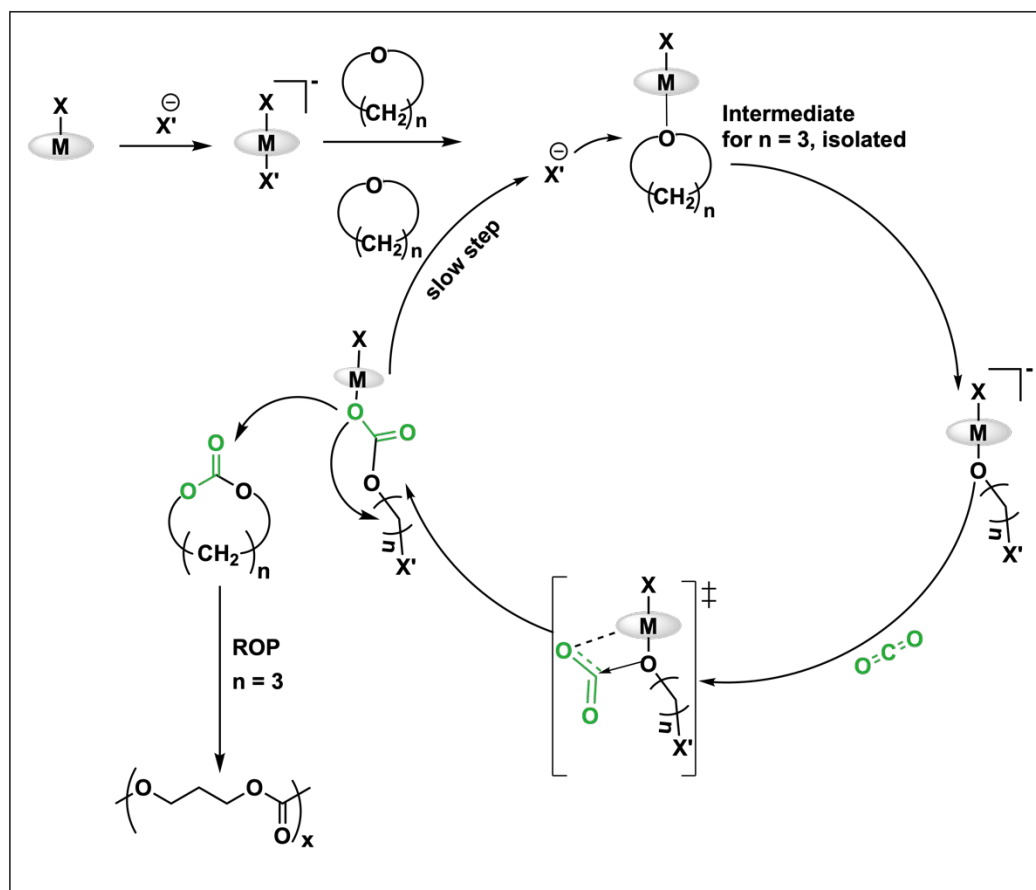
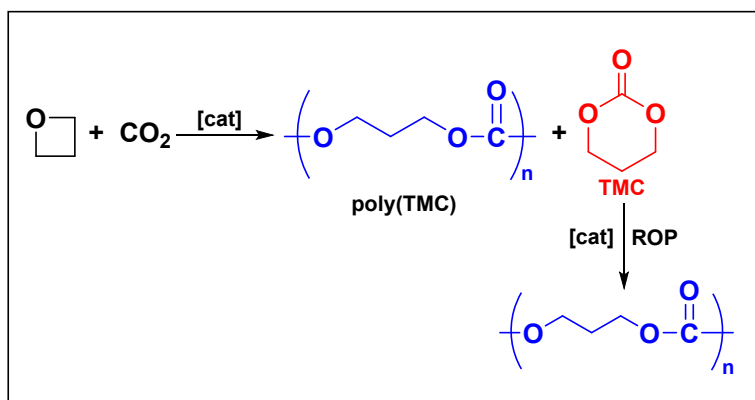


Figure 1. Catalytic cycle for the coupling of epoxides or oxetane and CO_2 where following the first cycle, $^{\ominus}X'$ represents the anionic growing polymer chain.

Hence, these observations clearly show much more rigorous conditions are required for the copolymerization of oxetane and CO₂, compared to that for epoxides and CO₂. This is somewhat unexpected since oxetane binds better to metal centers (more activated), and the energy released upon ring-opening of epoxides and oxetanes are similar. Notwithstanding, in the presence of a given metal catalyst, much higher temperatures are necessary for the copolymerization of oxetanes and CO₂. This in turn necessitates metal catalysts which are stable at these increased reaction temperatures. As mentioned earlier, whereas both oxetanes and oxiranes coupling reactions with CO₂ can provide varying quantities of cyclic carbonate products, in the case of oxetanes, these products are generally easily ring-opened by the same catalyst systems to their linear polymers (**Scheme 1**). An added greenness factor to these polycarbonate syntheses is that many oxiranes and oxetanes are liquids at ambient temperature, thereby allowing these copolymerization processes to be prepared in CO₂ expanded monomers without the need for organic solvents. In the following section, we will discuss the development of catalysts for the coupling of CO₂ and oxetanes.

Catalysts Development for the Coupling of CO₂ and Oxetanes

Various catalyst systems have been developed for the coupling of CO₂ and oxetanes to selectively produce either polycarbonates or cyclic carbonates. Similarly, there has been much activity aimed at designing catalysts for the ring-opening polymerization (ROP) of six-membered

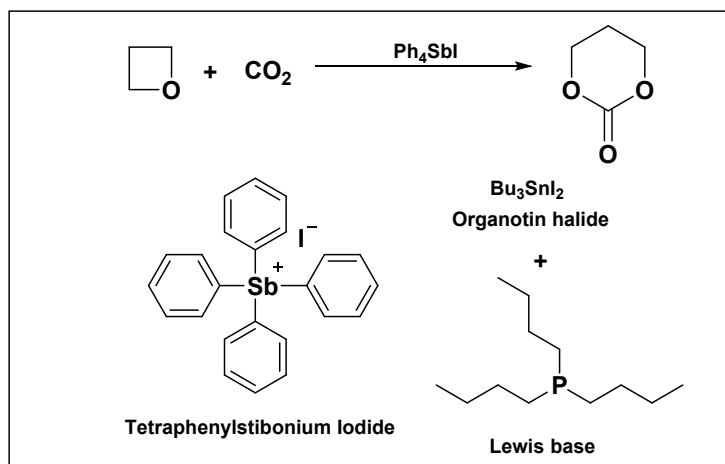


Scheme 1. General approach showing synthesis of poly(TMC) and trimethylene carbonate (TMC) which in turn can be opened to poly(TMC).

cyclic carbonates to afford the corresponding linear polycarbonates. The progression of catalysts which are effective at coupling CO₂ and oxetanes will be described below.

Catalysts for the Coupling of CO₂ and Oxetanes to Produce Cyclic Carbonates and their Ring-Opening Polymerization to Polycarbonates

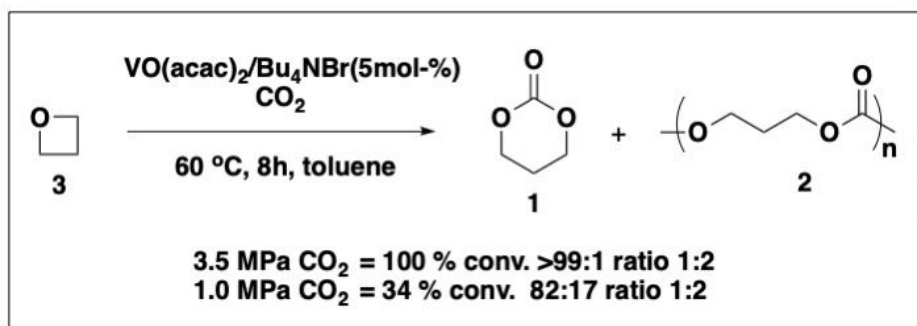
Although, there are innumerable publications documenting the catalytic coupling of CO₂ and epoxide to provide cyclic carbonates,^{12, 19, 36-40} there are limited reports of the catalysis of CO₂ and oxetanes to selectively provide cyclic carbonates. In part, this is due to the lower reactivity of the two cyclic ethers, and to the less selectivity of oxetanes and carbon dioxide to yield cyclic products. In spite of that, the selectivity and reactivity of four-membered ether rings with CO₂ can be modulated by exploring various catalysts and optimizing the reaction conditions. The first metal catalyzed coupling of oxetane and CO₂ was reported by Hirai and coworker at the University of Tokyo.⁴¹ These researchers were motivated by their earlier studies involving an organoaluminum based catalyst for the coupling of epoxides and CO₂.⁴² In this inquiry, the polymerization of oxetane and CO₂ was examined employing a ternary catalyst system composed of triethylaluminum, water, and acetylacetone in a ratio of 2:1:1 resulting in polymer formation in low yield with extensive ether linkages. Several years later in 1984, slightly better success was achieved by Baba and coworkers utilizing organotin halides in the presence of Lewis bases, such as phosphines or amines, as catalytic systems for the coupling of oxetane and CO₂ which resulted in low molecular weight polycarbonates.⁴³ The following year this group reported the first 1:1 cycloaddition of oxetane and CO₂ to selectively afford trimethylene carbonate (TMC) using a tetraphenylstibonium iodide catalyst as illustrated in **Scheme 2**.⁴⁴ However, the reaction required a temperature of 100 °C and CO₂ pressure of 4.9 MPa.



Scheme 2. Examples of catalytic systems employed by Baba for the coupling of oxetane and CO₂.

Baba research group further conducted more exhaustive studies on oxetane coupling with CO₂ by using a binary catalyst system of organotin iodides with phosphines or phosphine oxides.⁴⁵ They established that the choice of ligand that coordinates to tin was crucial and affects the catalytic activity and selectivity. For example, complexes formed by coordination of an organotin compound with Bu₃P produced polycarbonates exclusively, whereas, the combination of Bu₃SnI with Bu₃P=O yielded only the cyclic product, TMC, in good yields. They further proposed a detailed mechanism for this coupling reaction which will be discussed later.

We have employed a binary catalyst composed of a [VO(acac)₂] (acac = acetylacetonate) complex along with various ammonium halide salts for the selective conversion of oxetane into TMC under less harsh reaction conditions (**Scheme 3**).⁴⁶ The complex VO(acac)₂ which is obtained readily from a biocompatible metal, acts as a Lewis acid to activate oxetane, whereas the onium salt *n*-Bu₄NBr provides the nucleophile for this ring opening process. This pathway for synthesizing TMC is much greener than that produced from 1,3-propanediol and diethylcarbonate. To understand this coupling in more detail, the progress of the reaction was monitored by *in situ* infrared spectroscopy employing reaction conditions which provided quantitative yield for TMC formation. The infrared traces for selective TMC formation as a function of time are shown in **Figure 2**. Further, it was also observed that more harsh reaction conditions were needed for the coupling of substituted oxetanes.



Scheme 3. Approach for the selective coupling of oxetane and CO₂ to form TMC.

Kleij and co-workers reported a highly chemoselective synthesis of six-membered cyclic carbonates by employing binary catalysts composed of aluminum and iron aminophenolate complexes along with *n*-Bu₄NBr (TBAB) as cocatalyst (**Figure 3**).^{47, 48} These catalysts require very mild reaction conditions, and with many functional oxetanes showing promising yields for the formation of their respective cyclic products. From these observations it can be concluded that

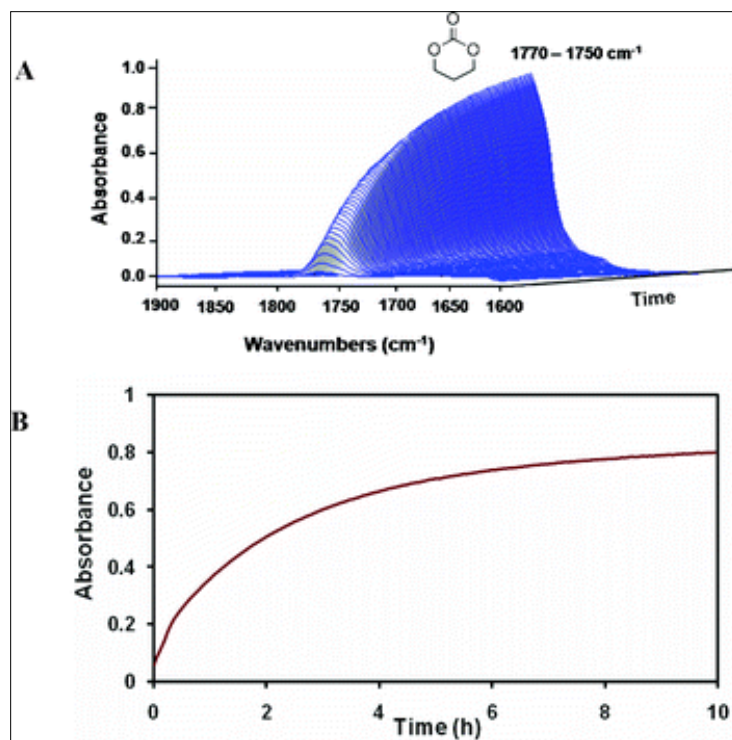


Figure 2. (A) Infrared spectra collected as a function of time for CO₂/oxetane coupling reaction.

(B) Trace for TMC formation at 60 °C and 3.5 MPa CO₂ in toluene.

organometallic catalysts for the formation of cyclic carbonates from substituted oxetanes have been developed, but the selectivity towards formation of the cyclic carbonate decreased significantly, with reaction times much longer for converting substituted oxetanes into the cyclic carbonates.

Wijayantha and coworkers have reported an electrochemical approach for the catalyst free synthesis of TMC selectively over its thermodynamically more stable poly(TMC) under atmospheric pressure of CO₂ and at ambient temperature (**Scheme 4**).⁴⁹ It was further demonstrated that when using tetrabutylammonium iodide as supporting electrolyte and 60 mA voltage, the selectivity for TMC over poly(TMC) can reach 99:1. This approach also showed promising results for substituted oxetanes, which required harsh reaction conditions when catalyzed by metal-based catalysts.

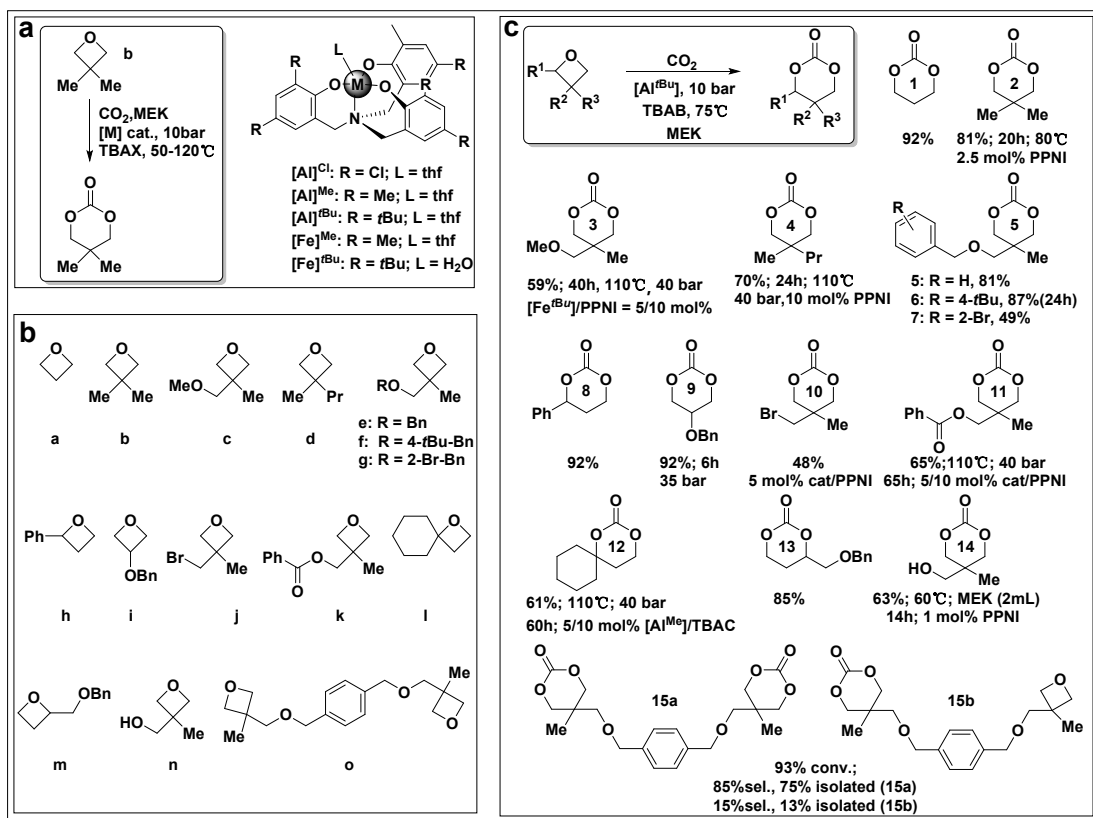
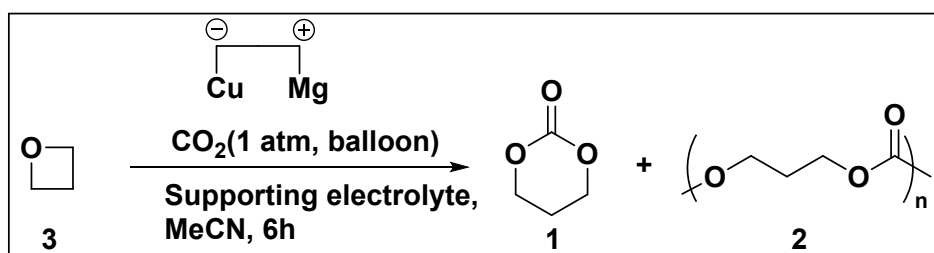


Figure 3. (a) Reaction scheme for the formation of six-membered cyclic carbonates with the structure of catalysts employed. (b) Structures of oxetane substrates employed in study (c) Six-membered cyclic carbonates produced with yields at 75 °C for 18 h reaction times.



Scheme 4. Electrochemical method for the selective synthesis of TMC over poly(TMC) at atmospheric pressure of CO_2 and ambient temperature.

Recently, Jérôme and coworkers reported for the first time a metal-free catalyst for the coupling of oxetane and CO_2 . The catalyst system consists of an onium salt and an alcohol which serves as hydrogen bond donor (HBD) (**Figure 4**).⁵⁰ The HBD, 1,3-bis-(hydroxyhexafluoroisopropyl)-benzene (1,3-bis-HFAB) was shown to be the most effective cocatalyst towards product selectivity and yields following optimization of reaction temperature

and pressure. Dove, Couleimber and coworkers employed equimolar mixture of iodine and a superbase, e.g., 1,8-diazabicyclo-[5.4.0]-undec-7-ene (DBU) to form TMC under 1 MPa CO₂ pressure. However, the obtained cyclic carbonate immediately polymerizes under reaction conditions into poly(TMC) through the activated chain-end mechanism, initiated from an I₂/oxetane adduct.⁵¹ More recently, the same research group has utilized a novel I₂-based binary organocatalytic approach of using iodine in combination with tetrabutylammonium acetate for coupling the oxetane and CO₂. In the presence of this catalytic system a common intermediate was proposed which upon changing the reaction temperature can preferentially lead to formation of either the six-membered cyclic TMC or poly(TMC).⁵² The cyclic product was obtained in 94% yield at 55 °C, whereas increasing the temperature to 105 °C led exclusively to the formation of poly(TMC). This temperature dependent approach provides a promising route for using less reactive oxetanes for the synthesis of either six-membered functional TMC or poly(TMC) using environmentally friendly organocatalysts.

At the time of this writing, another metal-free catalyzed reaction of oxetanes and carbon dioxide was reported.⁵³ That is, the coupling reaction of oxetane with CO₂ in the presence of alkyl boranes along with various nucleophiles was investigated at a CO₂ Pressure of 1.0 MPa and 90 °C. The order of reactivity with respect to the nucleophile was I⁻ ≈ Br⁻ > Cl⁻, with selectivity for formation of trimethylene carbonate being I⁻ > Br⁻ > Cl⁻. Although, onium chloride salts were selective for producing poly(TMC), 79 to 85 % in the cases of PPNCl and NBu₄Cl, the use of NBu₄N₃ exclusively provided poly(TMC) consistent with azide being a poorer leaving group than chloride. Furthermore, it was shown that the polymer was not derived from the ROP of TMC based on kinetic studies backed up by DFT computations. Interestingly, like noted for metal catalyzed direct production of copolymer from oxetane and CO₂, the afforded polymers possessed ether linkages. The activation parameters for trimethylene carbonate production from TMO and CO₂ in the presence of triethylborane and NBu₄I catalysts were determined to be $\Delta H^\ddagger = 28.0 \pm 5.0$ kcal/mol and $\Delta S^\ddagger = -238.5 \pm 16.7$ J/mol.K. The involvement of alkylboranes in activating TMO for ring-opening in the coupling reaction with CO₂ was supported by DFT computations. Consistent with studies of oxetane and CO₂ coupling reactions catalyzed by metal complexes, the substituted oxetane, 3,3- dimethyl oxetane was less reactive requiring higher reaction temperatures of 110 °C.

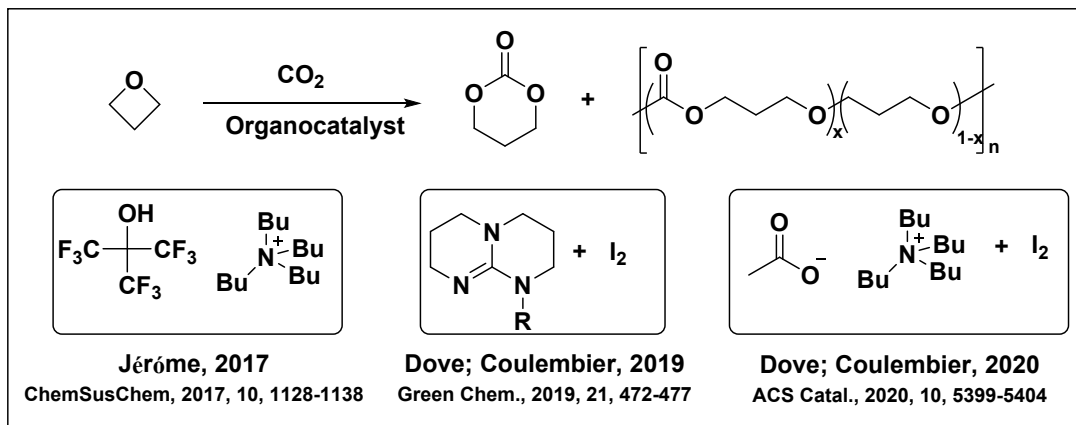


Figure 4. Coupling of CO₂ with oxetane catalyzed by different organocatalysts.

ROP of cyclic carbonates is an alternative strategy to produce aliphatic polycarbonates. As mentioned earlier, ring opening of five-membered cyclic carbonates like propylene carbonate to poly(propylene carbonate) is thermodynamically unfavorable, and is accompanied by loss of CO₂, and hence results in significant proportion of ether linkages in the resulting polycarbonates. The ROP of six-membered cyclic carbonates *via* TMC to poly(TMC) has been extensively investigated using a variety of catalysts. Initially cationic and anionic initiators have shown promising results for ROP of six-membered cyclic carbonates.⁵⁴⁻⁵⁹ The cationic initiators in the form of strong Lewis acids undergo cationic initiation producing poly(TMC) with a sizable proportion of ether linkages due to decarboxylation side reactions, whereas bases like alkoxides or alkyl lithium reagents initiate anionic ROP and produce polycarbonates with 100 % carbonate linkages.

Another strategy for the ROP of six-membered cyclic carbonates is based on a coordination-insertion mechanism. When catalysts, e.g., metal alkoxides having available sites for substrate binding, a two-step coordination insertion mechanism can be operational for ROP.⁶⁰ The initial step involves monomer binding which facilitates the ring-opening of the acyl-oxygen bond as illustrated in **Figure 5**. Tin(II)*bis*(2-ethyl-hexanoate) has been shown to be very effective catalyst for this process, producing polycarbonates with high molecular weights devoid of ether linkages (**Figure 5**).⁶¹

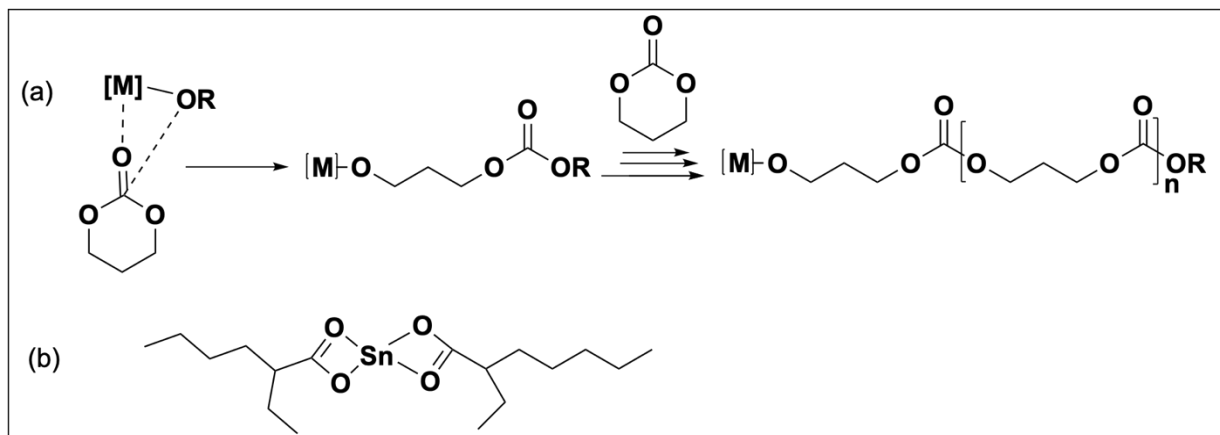


Figure 5. (a) Mechanism of metal-catalyzed ROP of TMC. (b) Structure of tin(II)*bis*(2-ethylhexanoate).

Tetraphenylporphyrin-aluminum complexes possessing chloride or methyl ligands in their fifth coordination sites were shown to be ineffective at catalyzing the ROP of 2,2-dimethyltrimethylene carbonate, whereas, complexes with more nucleophilic alkoxy ligands were efficient catalysts for this process (**Figure 6**).⁶² The polymerization reactions were found to be dependent on the reaction medium, with non-coordinating solvents showing better activity. Others, including Cao and Darensbourg research groups have shown aluminum salen complexes serve as excellent catalysts for the ROP of TMC. For example, Cao and coworkers have reported the ROP of TMC employing an aluminum catalyst with greater than 95 % conversion to afford poly(trimethylene carbonate) with a $M_w = 13,400$ Da and $\bar{D} = 1.41$.⁶³ Similarly, we have utilized a (salen)Al-OEt complex which displayed good activity ($\text{TOF} = 105 \text{ h}^{-1}$) to provide a polycarbonate with $M_w = 24000$ Da and $\bar{D} = 1.61$.⁶⁴

Inspired by catalytic studies of lactide polymerization, we have employed biometal salen complexes of Ca, Mg and Zn as catalysts for the ROP of TMC to poly(TMC), with the catalytic activity varying with metal in the order $\text{Ca}^{2+} > \text{Mg}^{2+} > \text{Zn}^{2+}$ (**Figure 7**).⁶⁵ Due to the lack of internal nucleophiles in these complexes, cocatalysts such as bis(triphenylphosphine)iminium chloride (PPNCl) were used to initiate the ring-opening process. Further these catalytic systems are of particular importance due to the biocompatible nature of metals, which eliminates the risk associated with the difficulty of removing trace amounts of metal residues from the produced polycarbonates. Similarly, Guillaume and coworkers have reported zinc complexes supported by a β -diiminate ligand along with benzyl alcohol as a chain transfer agent for the ROP of TMC

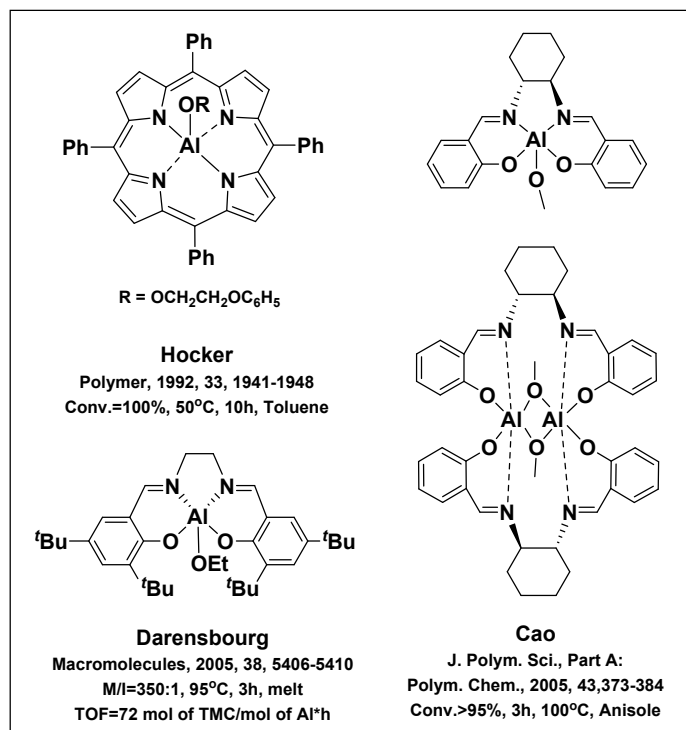


Figure 6. Examples of aluminum-based catalysts for ROP of TMC.

to poly(TMC).⁶⁶ This catalytic route offers unprecedented and efficient catalytic activities and productivities for the controlled “living” and “immortal” ROP of TMC, which allows for the growth of several polymer chains per metal center without loss of activity. Furthermore, with the same aim of using low toxic catalysts, acetylacetonates complexes of iron and zinc have also been reported as active catalysts for ROP of six-membered cyclic carbonates to poly(TMC) with zinc-based complex showing better activity compared to iron.⁶⁷ Other catalysts such as homoleptic lanthanide amidinate complexes,⁶⁸ samarium borohydride complexes,⁶⁹ lanthanide aryloxide complexes,⁷⁰ and 2,2-dibutyl-2-stanna-1,3-oxepane⁷¹ have also been employed as catalysts for the ROP of TMC.

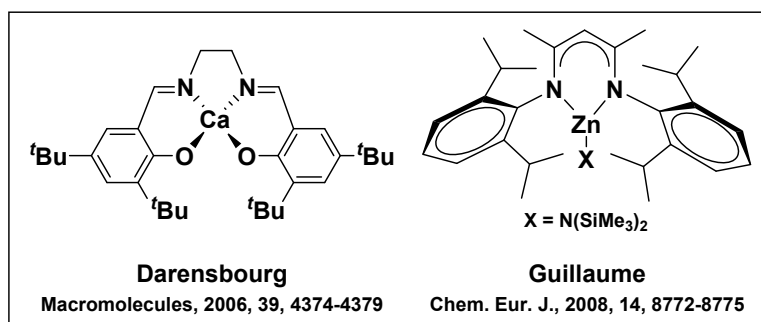
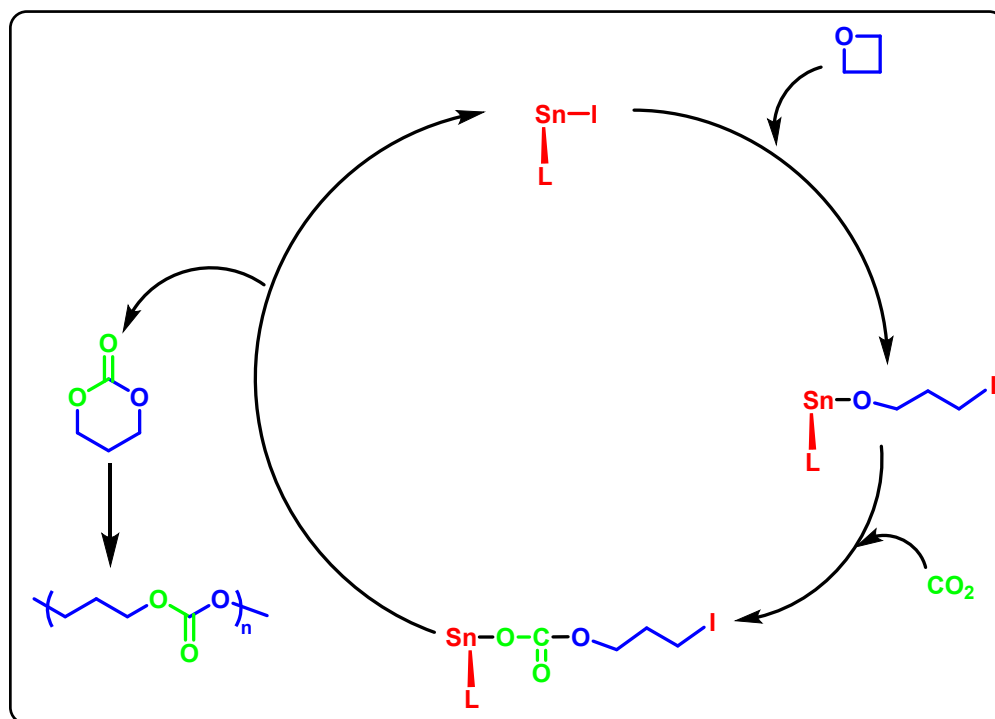


Figure 7. Examples of biometal-based catalysts used for the ROP of TMC to poly(TMC).

Catalysts for the Copolymerization of CO₂ and Oxetane, including Mechanistic Features of these Processes

Baba and coworkers proposed a mechanism for the formation of poly(TMC) and suggested that formation of TMC occurs initially, which later undergoes ROP to produce poly(TMC) (Scheme 5).⁴³ In the initiation step, the oxetane ring is opened by an organotin iodide complex producing an organotin iodopropoxide intermediate, which further undergoes CO₂ insertion into the Sn-O bond, to generate an organotin carbonate adduct. The catalyst is regenerated by the formation of TMC following backbiting. The Sn-I bond was found to be more nucleophilic, and hence activated for oxetane ring-opening, by the binding of phosphine or phosphine oxide to the tin center. Ring-opening of the preformed TMC was proposed to be catalyzed by the free-organotin iodide complex. Consistent with this mechanism was the observation that large excesses of phosphine oxide greatly retarded the rate of TMC polymerization since its dissociation is required for TMC binding. On the other hand, because phosphine binding to tin is weak, the presence of excess phosphine has no effect on the polymerization process.



Scheme 5. Reaction mechanism for copolymer formation proposed by Baba.

In 2001 Huang and coworkers reported rare earth metal complexes tri(2,6-di-*tert*-butyl-4-methylphenolate) ($\text{Ln}(\text{OAr})_3$, $\text{Ln} = \text{La}, \text{Nd}, \text{Dy}, \text{Y}$) as active catalysts for the ROP of 2,2-dimethyltrimethylene carbonate (DTC) to the corresponding polycarbonate which was produced without any ether linkages.⁷² These researchers further proposed that ROP occurs *via* a coordination anionic mechanism with ring opening occurs by acyl-oxygen bond cleavage. In our laboratory we later reported salen derivatives of Al(III) and Sn(IV) as effective catalysts for ROP of TMC to poly(TMC).⁶⁴ The optimization studies of these salen derivatives revealed that the most active catalysts in each instance contained a phenylene backbone with electron withdrawing, sterically unencumbered chloro substituents in the 3,5-positions of the phenolate rings, with the aluminum derivatives significantly more active than their tin(IV) counterparts. The mechanistic details revealed that ROP follows first order dependence on both [catalyst] and [monomer] and ¹H NMR studies of a low molecular weight poly(TMC) terminated by 2-propanol demonstrated that TMC ring-opening occurs by acyl oxygen bond cleavage as previously reported (**Figure 8**). A similar mechanism involving acyl oxygen bond cleavage rather than alkyl-oxygen bond cleavage during the ring opening of TMC was also proposed later by Huang and coworkers by employing lanthanide amidinate complexes $[\text{CyNC}(\text{R})\text{NCy}]_3\text{Ln}$ as catalysts for this reaction.⁷²

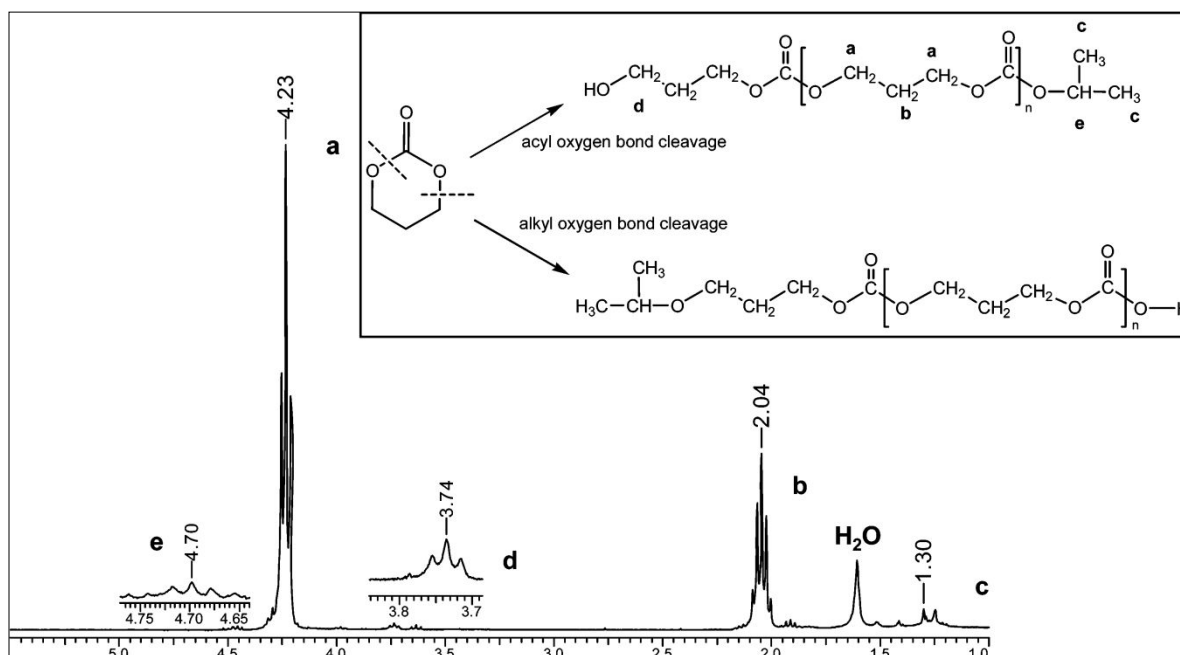
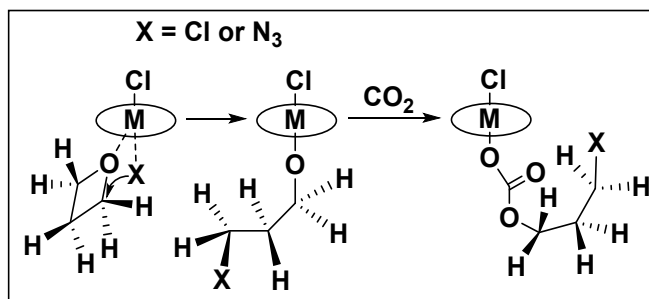


Figure 8. ¹H NMR spectrum of sample of poly(TMC) terminated by 2-propanol and ring-opening modes of TMC.

We have utilized binary metal salen derivatives of chromium and aluminum, along with n -Bu₄NX (X = Cl or N₃) salts, as selective catalysts for the coupling of oxetane and CO₂ to form poly(TMC) with only trace quantities of the TMC.⁷³ Further, it was observed that under all conditions Cr(III) derivatives were more active than their Al(III) analogues for copolymer formation. From a mechanistic perspective based on circumstantial evidence, the formation of copolymer was suggested to proceed directly rather than by the intermediacy of TMC as proposed previously by Baba and coworkers.⁴³ It was shown by both matrix-assisted laser desorption ionization time-of-flight (MALDI-TOF) mass spectrometry and infrared spectroscopy that the polymerization reaction catalyzed by (salen)Cr(III)Cl in the presence of n -Bu₄NN₃ as the cocatalyst, affords a polymer with an azide end group, suggesting the initiation step as first-order with respect to both (salen)Cr(III)Cl and n -Bu₄NX (**Scheme 6**).



Scheme 6. Mechanistic details during the coupling of CO₂ and oxetane suggesting initiating steps as first order with respect to both (salen)Cr(III)Cl and n -Bu₄NX.

Later, in studies designed to shed more light on the mechanism of this reaction, we have optimized the (salen)CrCl catalytic system for this coupling reaction using kinetic and copolymer end-group analysis employing *in situ* infrared and ¹H NMR spectroscopic techniques.^{34, 74} The binary catalyst system composed of (salen)CrCl with different cocatalysts have revealed that combinations having azide salts as cocatalysts show better activity than their chloride analogues. It has also been observed that these binary catalysts are quite selective towards poly(TMC) formation with selectivity varying with the cocatalyst anion as summarized in the **Table 1**. The diimine backbone of the (salen)CrX complex was varied, while maintaining the di-*tert*-butyl substituents in the 3,5-positions of the phenolate ring and exhibited little effect on catalytic activity. However, varying the groups on the phenolate ring while maintaining the phenylene

backbone of the salen ligand, revealed the bulky di-*tert*-butyl groups afford the more active catalyst. More insight into the mechanism of this coupling will be discussed below.

Table 1. Selectivity for Copolymer Formation using Complex **1** in the Presence of Various Cocatalysts.^a

Entry	Cocatalyst	% TMC ^b	%Poly(TMC) ^b	% Ether Linkages ^b
1	<i>n</i> -Bu ₄ NCl ^c	0	100	3.0
2	<i>n</i> -Bu ₄ NN ₃ ^c	0	100	2.9
3	<i>n</i> -Bu ₄ NBr	11.7	88.2	7.2
4	PPNCl	5.9	94	3.6
5	PPNN ₃	2.3	97.6	1.4
6	P(Cy) ₃	21.1	79	21.5

^a Copolymerization conditions: 17 mg of catalyst (0.15 mol%), 1.15 g of oxetane, M:I = 675:1, 2 equiv. of cocatalyst, 10 mL of toluene, 3.5 MPa of CO₂, at 110 °C for 24 h. ^b Product distributions were determined by ¹H NMR spectroscopy. ^c Previous published results. Note for the first three entries in Table 1 in reference 25, the % TMC is incorrectly reported due to misassigned ¹H NMR resonances.

Substrate Binding and Ring-Opening Steps of CO₂/Oxetane Coupling Examined by Infrared Spectroscopy

As mentioned earlier, the initiation step of the coupling reaction of CO₂ and oxetane in a common catalyst system occurs at a greatly reduced rate compared to the CO₂/epoxide process. In an effort to better define the CO₂/oxetane coupling process, we have utilized infrared spectroscopy to examine the oxetane binding and ring-opening steps using the (salen)CrN₃/PPNN₃ catalyst system.³⁴ The azide derivative is used because of the strong ν_{N_3} stretching vibration which provides a probe for both oxetane coordination to chromium and the oxetane ring-opening. Upon adding one equivalent of *n*-Bu₄NN₃ to (salen)CrN₃, (salen)Cr(N₃)₂ is readily formed at ambient temperature (**Figure 9a**). The six-coordinate complex has also been characterized in the solid-state by X-ray crystallography (**Figure 9c**). Evidence for the formation of the *bis*-azide complex in solution comes from the ν_{N_3} band 2083 cm⁻¹ of (salen)CrN₃ shifting to 2047 cm⁻¹ upon addition of *n*-Bu₄NN₃. Followed by the addition of excess oxetane to the *bis*-azide derivative, an increase in the ν_{N_3} vibration of free azide is observed at 2009 cm⁻¹ along with a decrease in ν_{N_3} of (salen)Cr(N₃)₂. Simultaneously, a new ν_{N_3} vibration at 2061 cm⁻¹ occurs which is assigned to the

(salen)Cr(N₃).oxetane complex (**Figure 9b**). The oxetane ring opening occurs upon heating this reaction mixture for three hours at 110 °C as evidenced by an organic azide band at 2100 cm⁻¹. The formation of an oxetane adduct with the salen metal complex prior to the ring opening process was confirmed by single crystal diffraction studies. Initial attempts to isolate the crystals of such adducts lead to the isolation of a hydroxo-bridged structure with oxetane bound to one of the chromium centers due to hydrolysis of Cr-Cl bond by trace quantities of water. On careful exclusion of water, successful isolation of single crystals of an oxetane adduct as depicted in the mechanistic **Scheme 8a** was obtained (**Figure 10**). Crystal structure analysis reveals that the dihedral angles of the planes C-O-C and C-C-C in the oxetane ligands were found to be 10.5° and 11.8° at 110 K. Hence, the oxetane molecule when bound to the metal center maintains its slight degree of nonplanarity similar to the metric parameters of the free monomer.⁷⁵

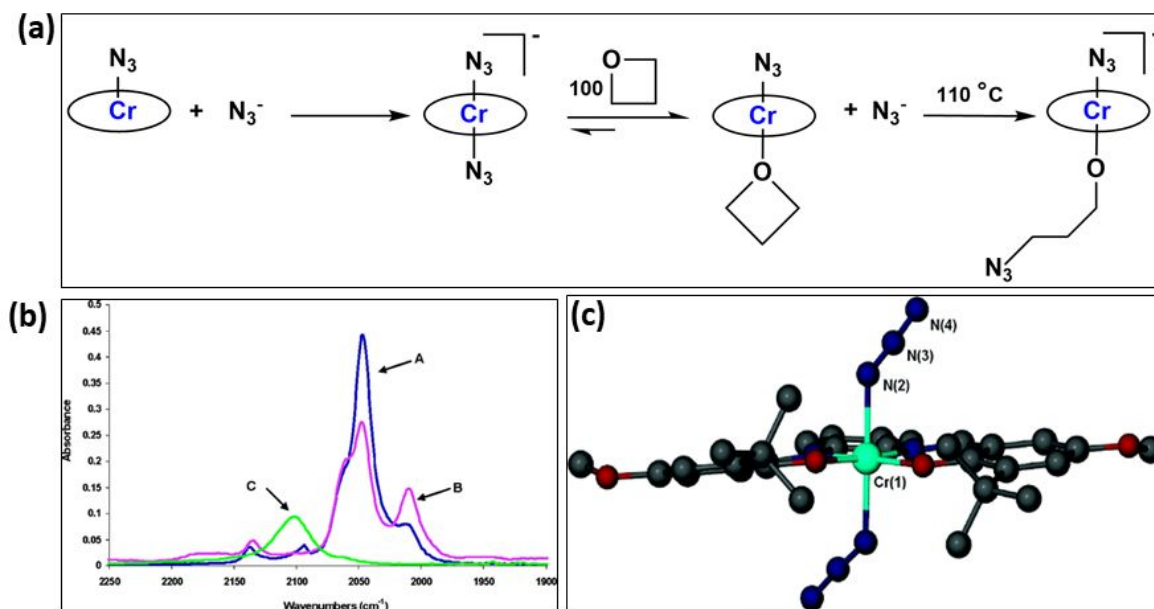


Figure 9. (a) Scheme showing formation of (salen)Cr(N₃)₂. (b) Spectra of 1,1,2,2-tetrachloroethane (TCE) solutions of (salen)Cr(N₃) with 1 equiv. of tetrabutylammonium azide (A), after the addition of 100 equiv. of oxetane at RT (B), and after heating the reaction soln. for 3 h at 110 °C (C). (c) X-ray structure of the anion of the [n-Bu₄N][(salen)Cr(N₃)₂] complex.

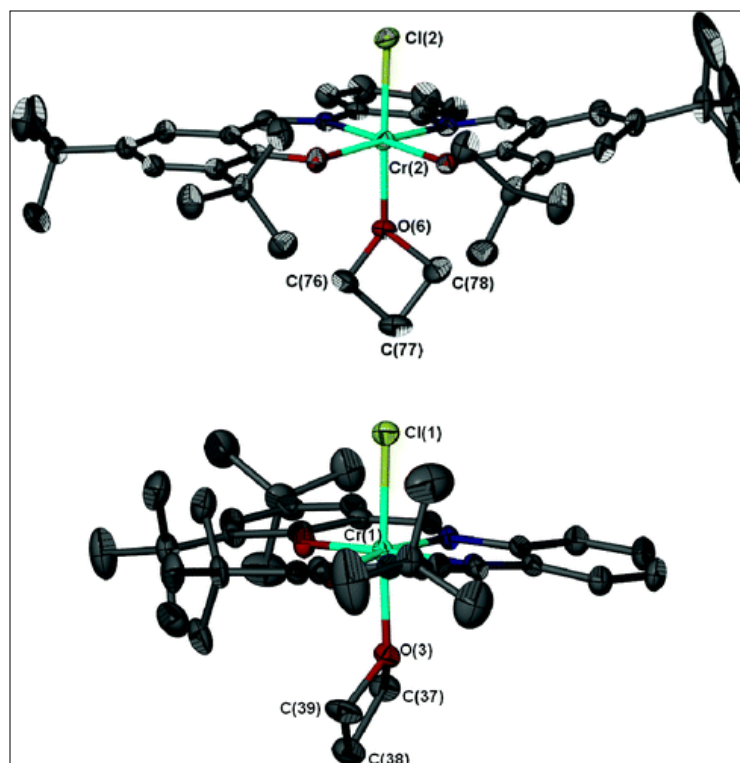


Figure 10. Crystal structure of chromium salen complex with bound oxetane.

Kinetic Studies of the Copolymerization of Oxetane and Carbon Dioxide

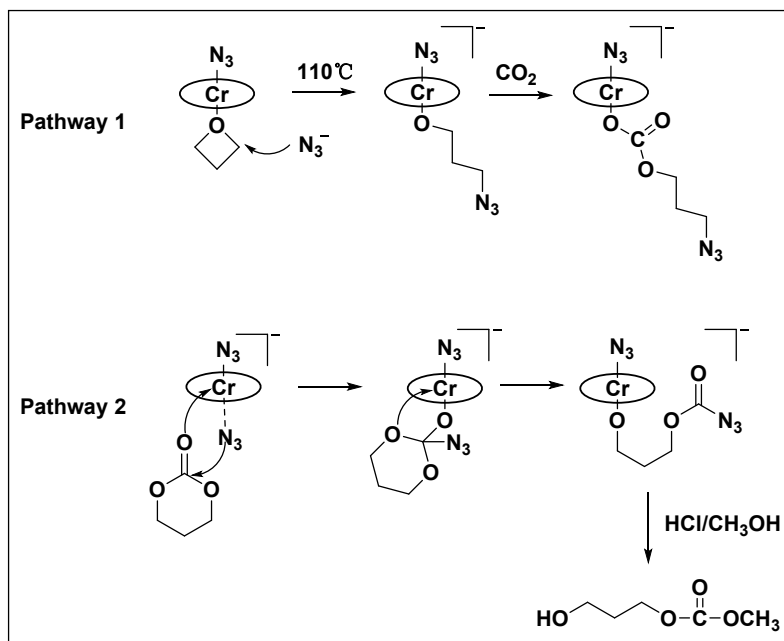
The kinetic studies of the coupling of oxetane and CO₂ were carried out by observing the growth of the copolymer, ν_{CO_2} band at 1750 cm⁻¹ as a function of time. It was shown that the intensity of this peak increases with time, and the reaction proceeds by first order kinetics with respect to both oxetane and catalyst concentrations. Further this coupling reaction follows first order dependence on the concentration of anionic initiator (cocatalyst) when used up to 2 equivalents, and zero order when used in excess such as 8 to 10 equivalents. As expected, the coupling reaction was found to be temperature dependent, and polymerization rate constants increased with increasing temperature from 80 to 110 °C. The calculated activation parameters ΔH^\ddagger was found to be 45.6 ± 3 kJ/mol, which is quite similar to that observed earlier for the copolymerization of cyclohexene oxide and CO₂ (45.5 kJ/mol) and lower than the process employing monomers such as propylene oxide and CO₂ (66.2 kJ/mol) with similar catalyst systems. The kinetic studies of the ROP of TMC to poly(TMC) were further carried out under comparable conditions as employed above. The log-log plots of the rate constant versus concentration of catalyst and cocatalyst reveals copolymerization reaction to be first order with

respect to both catalyst and cocatalyst. In order to understand the effect of temperature the ROP reaction was carried over the temperature range 105–130 °C. The activation parameters ΔH^\ddagger and ΔS^\ddagger calculated from the Eyring plot were found to be 74.1 ± 3.0 kJ/mol and -72.3 ± 2.3 J/mol·K respectively. These values are consistent with a reaction pathway involving the attack of a nucleophilic center (polymer chain end) to a metal-bound cyclic carbonate, with a ΔG^\ddagger value of 101.9 kJ/mol at 110 °C for the ROP of TMC. This is quite similar to the comparable ΔG^\ddagger value found for the copolymerization of oxetane and CO₂ (107.6 kJ/mol), suggesting that the two processes are energetically similar. These results thus conclude that polycarbonate formation from oxetane and CO₂ coupling occurs *via* two different or concurrent pathways, by formation of TMC intermediate followed by ROP or direct enchainment of oxetane and CO₂.

Further Mechanistic Insights into the Oxetane and Carbon Dioxide Coupling Process from ¹H NMR and End Group Analysis

The role of TMC was examined during the coupling of CO₂ and oxetane to produce copolymer by examining the reaction products as a function of time. This was accomplished by quenching aliquots removed from the reactor and assaying for products formed by ¹H NMR. The initial samples taken revealed the formation of TMC, with no TMC observed after four hours. Hence, at least a portion of the copolymer arises from the ROP of TMC. Combining this observation with polymer end-group analysis and the presence of some ether linkages in the copolymer, led us to conclude that copolymer formation occurs *via* ROP of TMC and oxetane/CO₂ alternating enchainment. Therefore, the two initiation pathways shown in **Scheme 7** take place subsequent to first generating traceable quantities of TMC by a back-biting process.

End group analysis on a low molecular weight polycarbonate obtained by the ROP of TMC revealed the presence of three types of end groups *viz* -CH₂OH, -OC(O)OCH₃ (confirmed by ¹H NMR) and an organic azide end group -CH₂N₃ (confirmed by ¹H NMR and FT-IR). There were no ether linkages observed during the ROP polymerization. The occurrence of -CH₂N₃ and -OC(O)OCH₃ end groups in the polymers obtained from TMC by ROP (**Figure 11**) is consistent with polymerization occurring *via* both acyl-oxygen and alkyl-oxygen bond cleavage modes, whereas previously it was reported that ROP occurs exclusively by an acyl-oxygen bond cleavage mode. Thus, the mechanism proposed for the copolymerization of oxetane and CO₂ under these



Scheme 7. Two different pathways during the coupling of oxetane and CO_2 .

experimental findings can be summarized in **Scheme 8**. As shown in the transition state, the azide may have some interaction with the Cr center during the initiation step. After the ring opening and

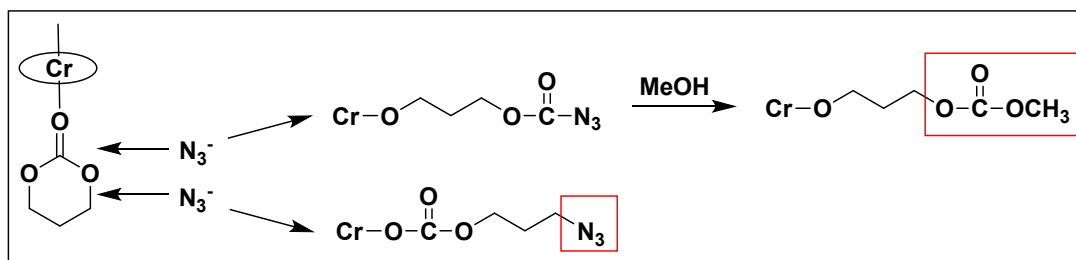
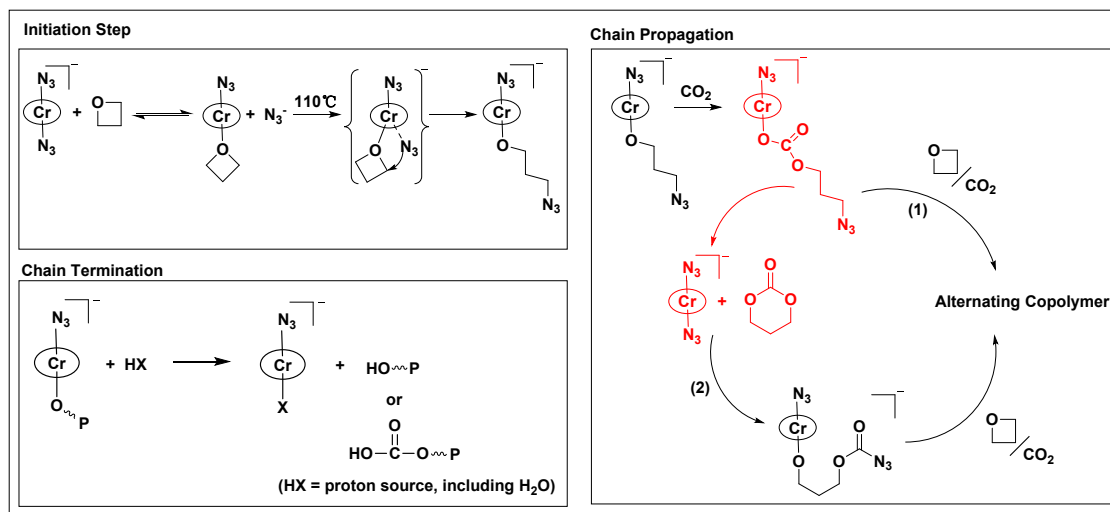


Figure 11. Ring opening of TMC occurring by both acyl-oxygen and alkyl-oxygen bond cleavage.

CO_2 insertion into the resultant chromium-oxygen bond, two routes are available for the intermediate. In route (1) consecutive additions of oxetane and CO_2 occurs leading to the formation of alternating copolymer, whereas route (2) produces TMC by a back-biting process with ring closure. The TMC produced can enter the copolymer chain by a coordination-insertion mechanism. The red portion of route (2) is highly depends on the nature of anionic leaving group. We have observed for bromide ion this pathway is competitive with oxetane enchainment and may

provide a mechanism for tuning the selectivity of the two pathways for poly(TMC) formation, where route (2) have the superiority of producing poly(TMC) without any ether linkages.



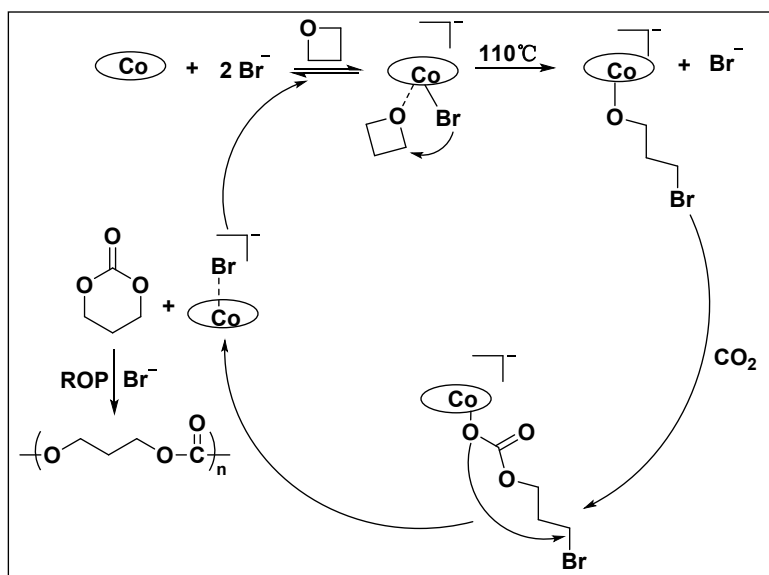
Scheme 8. Mechanism for the coupling of oxetane and CO_2 catalyzed by binary $(\text{salen})\text{CrN}_3/n\text{-Bu}_4\text{NN}_3$ catalytic system.

Recent Advances in Understanding the Mechanistic Aspects of Oxetane and Carbon Dioxide Coupling

Previously we have surmised that the selectivity for TMC or poly(TMC) formation can be tuned by decreasing the electrophilicity of the metal center in conjunction with the appropriate anionic initiator. In order to validate this hypothesis, we have employed binary catalytic systems composed of commercially available $(\text{salen})\text{Co}(\text{II})$ in presence of anionic-based cocatalysts derived from $n\text{-Bu}_4\text{NX}$ salts.⁷⁶ The choice of $(\text{salen})\text{Co}(\text{II})$ was made due to its reduced electrophilicity and substitutional lability relative to $(\text{salen})\text{CrX}$ complexes. The catalytic studies revealed that both cyclic TMC and poly(TMC) products were obtained and catalytic activity depends on the anion of the cocatalyst employed, with the order of decreasing activity being $\text{Br}^- > \text{I}^- > \text{Cl}^- > \text{N}_3^-$. Similar trends have been observed by Endo utilizing alkali metal- or tetraalkylammonium-halides catalysts for CO_2 or CS_2 coupling reactions with aziridines.⁷⁷ The selectivity for poly(TMC) products in instances where the cocatalysts have Br and I anions is very high compared to cyclic TMC. In order to understand the effect of cocatalysts(anion) the copolymerization reaction was carried out using the $(\text{salen})\text{Co}(\text{II})/n\text{-Bu}_4\text{NBr}$ catalytic system in

toluene. Solution state *in situ* infrared spectroscopy was employed to monitor the reaction by observing the growth of the copolymer's ν_{CO_3} band at 1750 cm^{-1} , as well as the growth and/or consumption of the TMC's ν_{CO_3} band at 1770 cm^{-1} . It was observed that the rate of poly(TMC) production was highest when 2 equiv. of *n*-Bu₄NBr was used, and when more than 2 equiv. of *n*-Bu₄NBr was used, production of TMC over that of poly(TMC) increases but the overall catalytic activity decreased.

These experimental findings were used to propose the mechanistic aspects for the coupling reaction of oxetane and CO₂ catalyzed by (salen)Co(II)/*n*-Bu₄NBr catalyst. Initially, formation of a (salen)Co(II)Br•(oxetane) occurs which facilitates the ring-opening of oxetane followed by CO₂ insertion into the resultant cobalt-oxygen bond which can undergo ring closure to form TMC with the regeneration of a (salen)CoBr species. The TMC produced can be further ring opened in the presence of bromide anion in solution to yield poly(TMC) (Scheme 9). Nevertheless, the role of cobalt(II) is not completely understood, i.e., is its only purpose to activate the monomer for ring-opening or does CO₂ insertion also occur into the Co-O bond. Alternatively, CO₂ addition to a dissociated alkoxide could be taking place.



Scheme 9. Summarized proposed mechanistic aspects for the coupling reaction of oxetane and CO₂ catalyzed by binary (salen)Co(II)/*n*-Bu₄NBr catalytic system.

These experimental findings inspired us to further explore the activity and selectivity of (salen)Cr(III)Cl in presence of cocatalysts $n\text{-Bu}_4\text{NX}$ with different anions ($X = \text{Br}, \text{I}, \text{Cl}, \text{N}_3, \text{NCO}$). Some of these anions are better leaving groups than azide for tuning the selectivity of oxetane and CO_2 coupling for TMC formation, and/or for poly(TMC) produced from the homopolymerization of preformed TMC.⁷⁸ Initially we have used binary catalyst systems composed of (salen)Cr(III)Cl with the various $n\text{-Bu}_4\text{NX}$ salts to examine the catalytic activity and product selectivity. The reactions were followed using *in situ* IR spectroscopy by monitoring the ν_{CO_3} bands at 1750 and 1770 cm^{-1} . The deconvoluted FT-IR spectra revealed that the rate of copolymer formation varies slightly with the nature of anion with the order $\text{Br}^-, \text{I}^- > \text{Cl}^-, \text{N}_3^- > \text{NCO}^-$. Similar to earlier report on (salen)Co(II) using the same anions, these studies also revealed that Br^- is more selective initially for the formation of TMC by the backbiting process, followed by iodide, chloride, azide, and cyanate anions. Reaction profile of a polymerization reaction catalyzed by 2 equivalents of $n\text{-Bu}_4\text{NBr}$ as cocatalyst revealed initially formation of TMC is enhanced and rapidly decreased over time, whereas poly(TMC) is slow initially but increases rapidly with time (**Figure 13**). The copolymerization reaction was performed at different temperatures and the experimental results revealed that selectivity for TMC formation due to backbiting mechanism increases as the reaction temperature was decreased from 110 to 60 $^\circ\text{C}$ whereas the catalytic activity for ROP should also decrease, but the formation of TMC and the production of polycarbonate through ROP of preformed TMC *via* a coordination-insertion mechanism is favored at lower temperatures. Electrospray ionization mass (ESI-MS) spectrometry studies suggested that on treatment of the (salen)CrCl with two equivalents of a bromide-based cocatalyst forms [trans-(salen)CrClBr⁻] which exists in solution in a Schlenk equilibrium with the corresponding symmetric [trans-(salen)CrX₂⁻] ($X = \text{Cl}$ or Br). The selectivity for TMC formation *via* back biting mechanism could also be tuned by using binary catalytic system (salen)CrCl/ $n\text{-Bu}_4\text{NBr}$ at lower reaction temperatures and CO_2 pressures.

Wijayantha and coworkers recently employed an electrochemical approach for the selective synthesis of TMC over poly(TMC) at atmosphere pressure of CO_2 and mild reaction condition.⁴⁹ Mechanistic studies revealed that the first formation of magnesium iodide occurs *in situ*, consistent with the report of North and coworkers⁷⁹ which suggested that tributylamine is released under the reaction conditions which in turn activates CO_2 towards incorporation into

cyclic TMC formation. This is accompanied by the regeneration of magnesium iodide (**Scheme 10**).

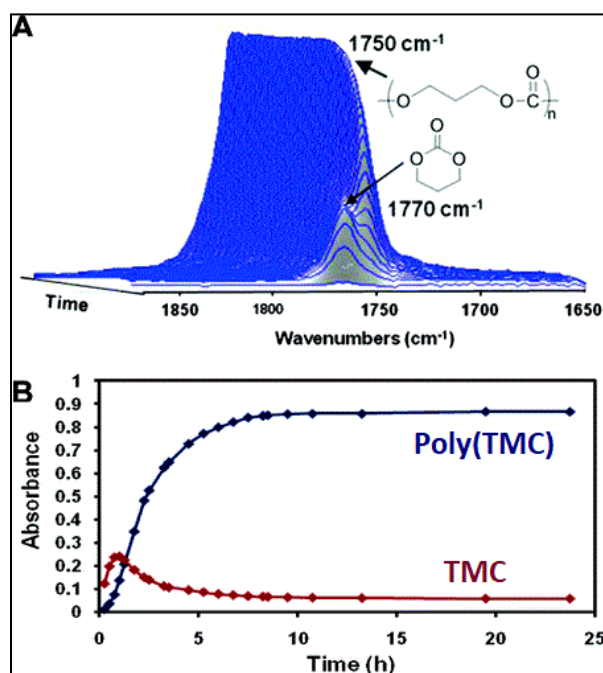
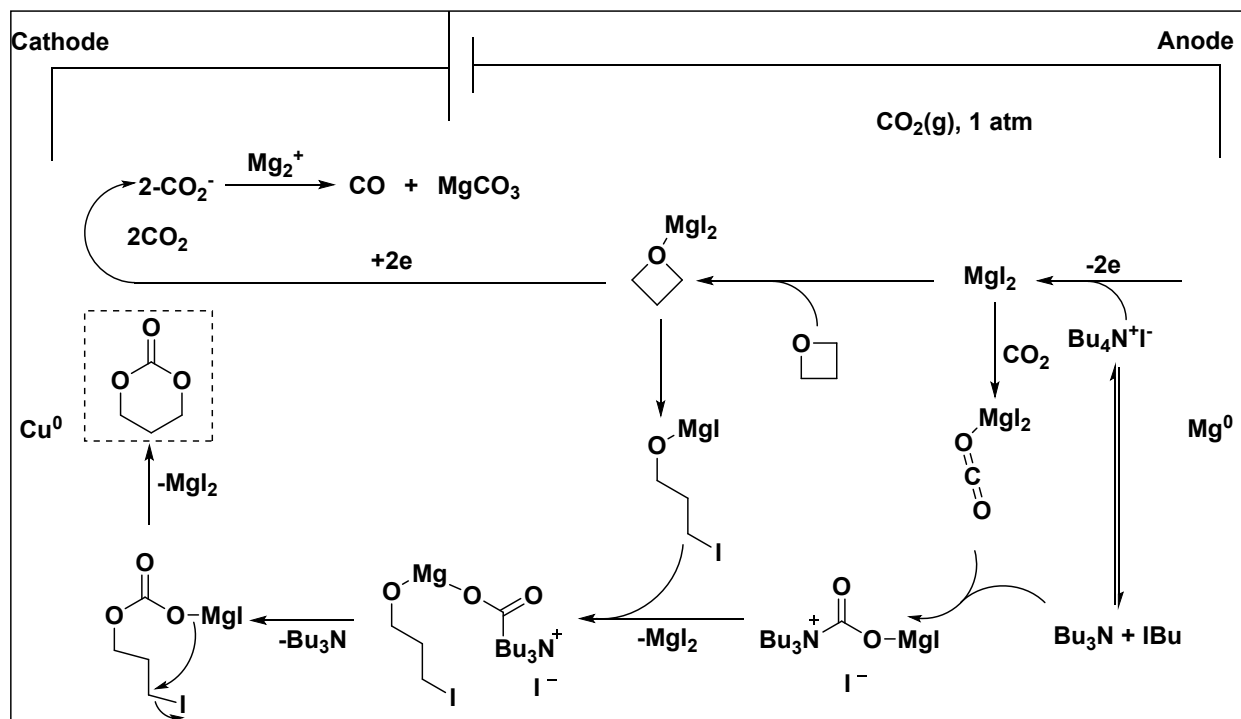
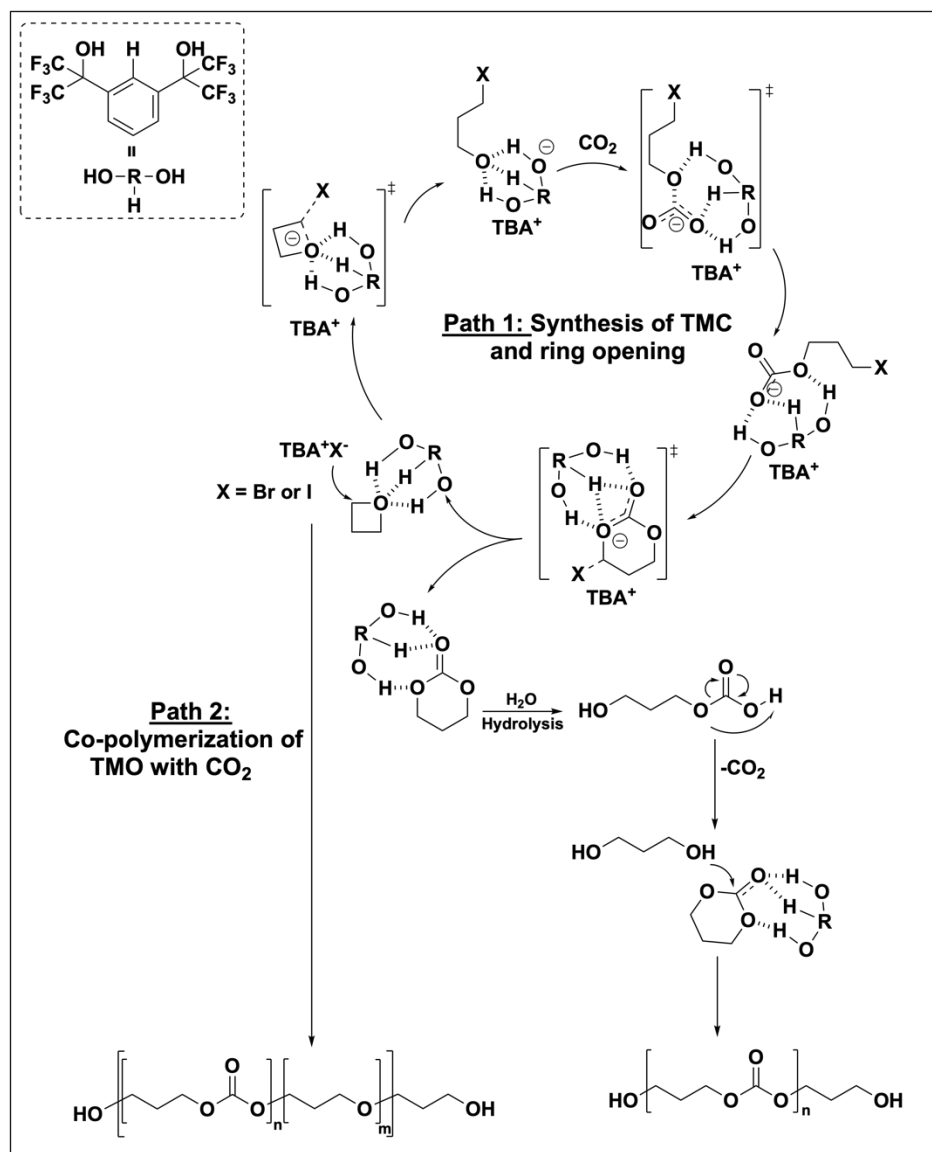


Figure 13. Reaction of oxetane and CO_2 catalyzed by $(\text{salen})\text{Co}(\text{II})$ in the presence of two equivalents of Bu_4NBr (A) Infrared spectra as a function of reaction time, with product traces shown in (B).⁷⁸



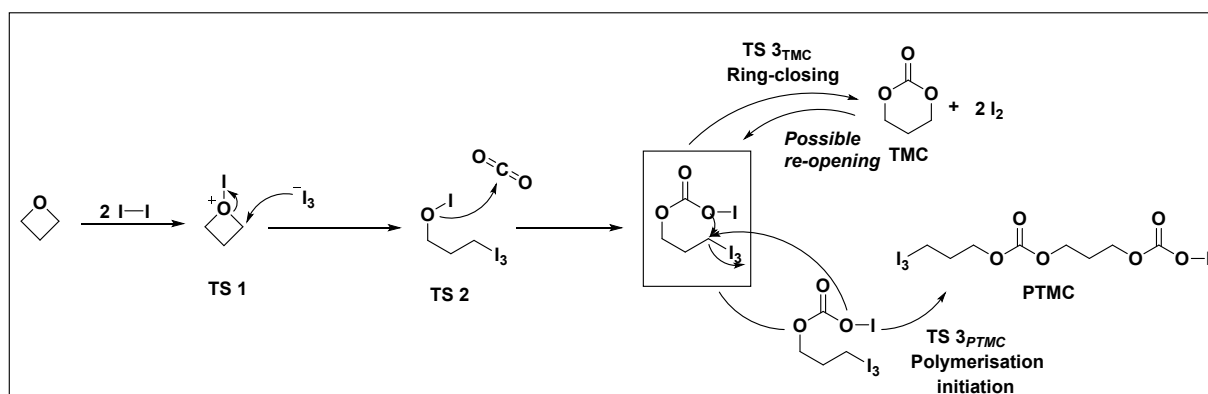
Scheme 10. Proposed mechanism for the formation of TMC using electrochemical approach.

In a unique approach, researchers have used a metal-free organocatalyst system composed of a tetrabutylammonium salt and a hydrogen bond donor (fluorinated alcohol) for the coupling of CO_2 and oxetane.⁵⁰ In order to better understand the mechanism of this catalytic process, a detailed kinetic study using online FT-IR combined with DFT calculations and ^1H NMR titrations concluded two mechanistic pathways for the formation of polymers either by ROP of TMC or by direct copolymerization of oxetane with CO_2 (**Scheme 11**).



Scheme 11. Mechanistic details proposed for the synthesis of oligocarbonates from oxetane/ CO_2 coupling catalyzed by the binary tetrabutylammonium iodide (TBAI)/1,3-bis-HFAB organocatalyst. $\text{RH}(\text{OH})_2$ represents 1,3-bis(2-hydroxyhexafluoroisopropyl)benzene.

Dove and coworkers have employed a binary catalyst system comprised of I_2 and tetrabutylammonium acetate (TBAAc) for the coupling of CO_2 and oxetane. They observed that product selectivity could be tuned for the formation of either TMC or its corresponding ring-opened polymer poly(TMC) by modulating the reaction temperature.⁵² Comprehensive kinetic studies supported by DFT calculations suggested that at higher temperatures product selectivity can be tuned for the formation of poly(TMC) either by the ROP of *in situ* formed TMC or by the direct coupling of CO_2 and oxetane (**Scheme 12**).



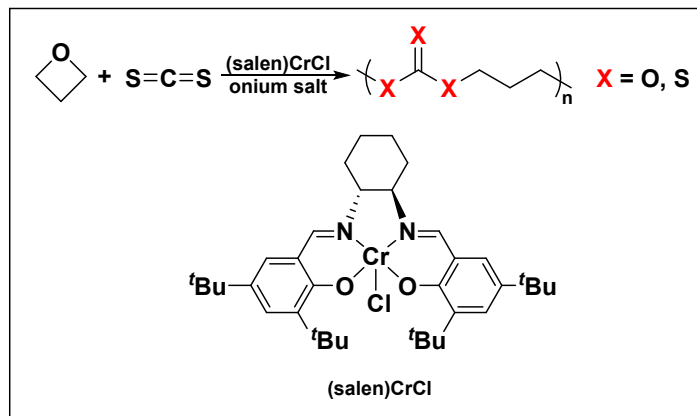
Scheme 12. Proposed mechanism for the coupling of CO_2 and oxetane catalyzed by iodine (I_2) and the two proposed pathways for the formation of TMC or Poly(TMC).

As mentioned earlier in this review, the majority of the coupling reactions of oxetanes and CO_2 are homogeneously catalyzed by well-defined metal complexes or organocatalysts. However, there are examples of heterogeneous catalysts for the coupling of CO_2 and cyclic ethers. For example, there is a report on the use of a supported hybrid heterogeneous organocatalysts based on imidazolium modified polyhedral oligomeric silsesquioxanes (POSS- I_{MI}) grafted on SiO_2 .⁸⁰ This solvent-free and recyclable process was shown to be 100 % selective for trimethylene carbonate production at 4 MPa of CO_2 150 °C

Recent Investigations of the Copolymerization of Oxetane with the Sulfur Analogues of CO₂

Carbonyl sulfide (COS) and carbon disulfide (CS₂) are sulfur analogues of CO₂ and have been proven to be very efficient sulfur-containing C1 building blocks to synthesize sulfur-containing polymers such as poly(thiocarbonate)s,⁸¹⁻⁸⁵ polythioureas⁸⁶ and polythiourethanes.⁸⁷ Similar to CO₂, COS and CS₂ have also been utilized as comonomer to copolymerize with oxetane, and recent research progress of these studies is briefly reviewed below.

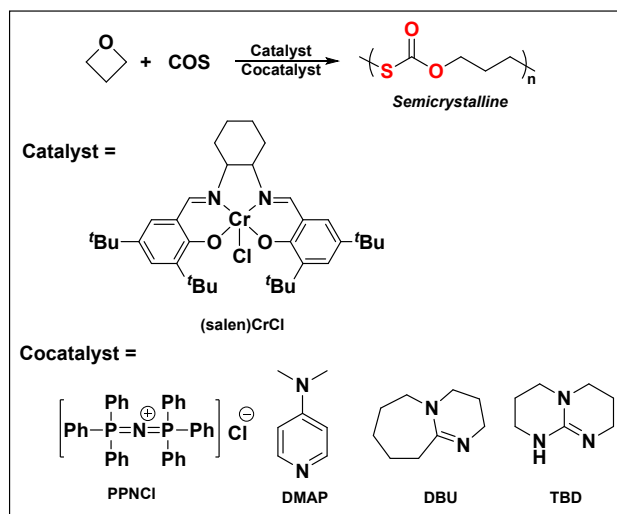
CS₂ has been proven to be a very reactive sulfur-containing building block to construct poly(thiocarbonate)s by copolymerizing with various three-membered ring epoxides.⁸⁹⁻⁹¹ However, inevitable oxygen/sulfur (O/S) exchange reaction occurred during the copolymerization process and resulted in random distribution of oxygen and sulfur atoms in both the poly(thiocarbonate)s and cyclic thiocarbonates products. The chain structure of the resulting polymeric products was not well-defined, and the mechanism of O/S exchange reaction was inadequately understood. Considering that oxetane has a symmetric four-membered ring structure, we utilized oxetane as a model compound to copolymerize with CS₂ in order to construct a relatively well-defined polymerization system to investigate the oxygen/sulfur scrambling.⁹² The CS₂/oxetane copolymerization was efficiently catalyzed by (salen)CrCl in conjunction with onium salt as shown in **Scheme 13**. Because of the symmetry of oxetane and CS₂, the signals of the products various structures did not overlap in the ¹H NMR spectra. These independent ¹H NMR peaks enabled the quantitative characterization of different thiocarbonates linkages and cyclic products for the first time. Five different thiocarbonates linkages and two cyclic thiocarbonates were well-characterized by ¹H and ¹³C NMR spectroscopy, and these results were further confirmed by *in situ* infrared spectroscopic monitoring of the reaction. This research provided a reliable basis for investigating the factors affecting O/S scrambling.



Scheme 13. Oxetane/CS₂ copolymerization catalyzed by (salen)CrCl and onium salt.

On the basis of CS₂/oxetane copolymerization, we carried out the copolymerization of oxetane with COS for the sake of suppressing O/S scrambling and achieving a well-defined poly(monothiocarbonate). As expected, a well-defined and fully alternating poly(trimethylene monothiocarbonate) was efficiently prepared by the copolymerization of COS with oxetane catalyzed by (salen)CrCl in conjunction with different organic bases (**Scheme 14**).⁹³ This copolymerization exhibited excellent selectivities, which was specifically manifested in that the O/S scrambling and the production of cyclic byproducts were well suppressed even at higher reaction temperatures (100 to 130 °C). Of importance, the characterization of the synthesized polymer showed that it exhibits spherulitic crystal morphology and has a melting temperature of 127.5 °C and a crystallinity of 71%, which is similar to high-density polyethylene. Unlike the CO₂/oxetane copolymerization system, the sulfur atoms introduced into the main chain promoted the regular arrangement of the polymer backbone when COS was used as a comonomer of oxetane. The crystallization behavior of these polymers does not rely on the chirality of the catalysts or monomers, but only on the regular arrangement of the polymer itself, which is quite special in the copolymerization systems of CO₂ and its sulfur analogues with epoxides and oxetanes. The same crystallization behavior was also observed on the copolymer of COS and ethylene oxide. Ren and coworkers reported a semicrystalline poly(monothiocarbonate) synthesized *via* the copolymerization of ethylene oxide with COS catalyzing by a bifunctional chromium(III) complex.⁹⁴ The synthesized copolymer was alternating and possessed a melting temperature of 128.2 °C. The mechanism of introducing sulfur atoms can promote crystallinity is still

inadequately understood. The investigation and revelation of this mechanism will benefit the design and construction of sulfur-containing semicrystalline polymeric materials.



Scheme 14. COS/OX copolymerization catalyzed by (salen)CrCl with different organic bases.

More recently, Zhang and coworkers have employed a binary organic catalytic system comprised of triethylborane and PPNCl for the coupling of COS and oxetane.⁹⁵ In that work, the researchers investigated the spherulitic crystal morphology and isothermal crystallization property of poly(trimethylene monothiocarbonate) prepared by the copolymerization of COS with oxetane. It was found that poly(trimethylene monothiocarbonate) tended to form banded spherulites, and this tendency was more intense at lower crystallization temperatures. With the help of small-angle X-ray scattering, the researchers proved that there were more amorphous phases located in the interlamellae of poly(trimethylene monothiocarbonate), and these factors led to larger long period (L) and thicker amorphous layers (l_a), which promoted poly(trimethylene monothiocarbonate) to form banded spherulites.

Conclusions

Presently, the coupling of CO₂ and three-membered cyclic ethers, oxiranes or epoxides, to selectively afford either completely alternating copolymers or cyclic carbonates, is in general a well-studied and widely developed strategy for valorization of carbon dioxide. Alternatively, analogous coupling reactions of CO₂ and four-membered cyclic ethers, oxetanes, are much less investigated. This is due in part to the limited and expensive availability of oxetane monomers from commercial sources. However, there are good synthetic methods for producing the most

commonly utilized oxetane, trimethylene oxide, which has important biomedical and pharmaceutical applications, such as absorbable sutures, drug delivery, and tissue engineering. Efforts are currently being directed at developing strategies for synthesizing numerous oxetane derivatives. Although, the ring-strain energies of oxiranes and oxetanes are comparable, and the binding ability of oxetanes to metal catalysts is stronger, the ring-opening of oxetanes by nucleophiles for initiation or chain growth processes requires more harsh conditions and more thermally stable catalysts than the corresponding reactions of epoxides. It is also noted herein that the direct coupling of oxetanes and CO₂ to copolymers can lead to small quantities of ether linkages in the thus afforded polycarbonates, whereas, the ring-opening polymerization of the corresponding cyclic carbonates provide completely alternating copolymers. In summary, recent developments in the area of polymeric materials synthesized from CO₂, or its sulfur analogs, with oxetanes could provide new applications for these polymers. Furthermore, akin to current efforts in epoxide/CO₂ copolymerization processes, future studies focusing on the use of oxetanes derived from renewable resources are warranted.¹⁷

* Corresponding Authors

Donald J. Darensbourg

Email: djdarens@chem.tamu.edu

Orcid: 0000-0001-9285-4895

Ming Luo

Email: mingluo@cslg.edu.cn

Orcid: 0000-0002-6166-0681

Declaration of interest

The authors declare no competing financial interest.

Acknowledgments

D. J. Darensbourg gratefully acknowledge the financial support of the National Science Foundation (CHE-1665258 and CHE-1610311) and the Robert A. Welch Foundation (A-0923). M. Luo gratefully acknowledge the financial support of Natural Science Foundation of China (21704007), Natural Science Foundation of Jiangsu Province (BK20170434).

References

1. E. S. Stevens, *Green plastics: an introduction to the new science of biodegradable plastics*, Princeton University Press, 2002.
2. B. C. Gibb, *Nat. Chem.*, 2019, **11**, 394-395.
3. R. Petrus and P. Sobota, *Coord. Chem. Rev.*, 2019, **396**, 72-88.
4. D. J. Darensbourg and M. W. Holtcamp, *Coord. Chem. Rev.*, 1996, **153**, 155-174.
5. G. W. Coates and D. R. Moore, *Angew. Chem. Int. Ed.*, 2004, **43**, 6618-6639.
6. H. Sugimoto and S. Inoue, *J. Polym. Sci., Part A: Polym. Chem.*, 2004, **42**, 5561-5573.
7. D. J. Darensbourg, R. M. Mackiewicz, A. L. Phelps and D. R. Billodeaux, *Acc. Chem. Res.*, 2004, **37**, 836-844.
8. M. H. Chisholm and Z. Zhou, *J. Mater. Chem.* 2004, **14**, 3081-3092.
9. D. J. Darensbourg, *Chem. Rev.*, 2007, **107**, 2388-2410.
10. S. Klaus, M. W. Lehenmeier, C. E. Anderson and B. Rieger, *Coord. Chem. Rev.*, 2011, **255**, 1460-1479.
11. M. R. Kember, A. Buchard and C. K. Williams, *Chem. Commun.*, 2011, **47**, 141-163.
12. X.-B. Lu and D. J. Darensbourg, *Chem. Soc. Rev.*, 2012, **41**, 1462-1484.
13. X.-B. Lu, W.-M. Ren and G.-P. Wu, *Acc. Chem. Res.*, 2012, **45**, 1721-1735.
14. D. J. Darensbourg and S. J. Wilson, *Green Chem.*, 2012, **14**, 2665-2671.
15. S. Paul, Y. Zhu, C. Romain, R. Brooks, P. K. Saini and C. K. Williams, *Chem. Commun.*, 2015, **51**, 6459-6479.
16. G. Trott, P. Saini and C. Williams, *Philos. Trans. Royal Soc.*, 2016, **374**, 20150085.
17. S. J. Poland and D. J. Darensbourg, *Green Chem.*, 2017, **19**, 4990-5011.
18. C. M. Kozak, K. Ambrose and T. S. Anderson, *Coord. Chem. Rev.*, 2018, **376**, 565-587.
19. A. J. Kamphuis, F. Picchioni and P. P. Pescarmona, *Green Chem.*, 2019, **21**, 406-448.
20. J. Huang, J. C. Worch, A. P. Dove and O. Coulembier, *ChemSusChem*, 2020, **13**, 469-487.
21. Y.-Y. Zhang, G.-P. Wu and D. J. Darensbourg, *Trends Chem.*, 2020, **2**, 750-763.
22. A. Pell and G. Pilcher, *Trans. Faraday Soc.*, 1965, **61**, 71-77.
23. T. L. Allen, *J. Chem. Phys.*, 1959, **31**, 1039-1049.
24. Sigmaaldrich.com, as of Oct. 15, **2020**
25. C. Derick and D. Bissell, *J. Am. Chem. Soc.*, 1916, **38**, 2478-2486.
26. C. Noller, *Org. Synth.*, 2003, **29**, 92-92.
27. S. Searles, *J. Am. Chem. Soc.*, 1951, **73**, 124-125.
28. A. A. Hullio and G. Mastoi, *Int. J. Chem.*, 2013, **5**, 57.
29. C. W. Forsberg, *Appl. Environ. Microbiol.*, 1987, **53**, 639-643.

30. A.-P. Zeng and H. Biebl, *Adv. Biochem. Eng. Biotechnol.*, 2002, 239.
31. C. E. Nakamura and G. M. Whited, *Curr. Opin. Biotechnol.*, 2003, **14**, 454-459.
32. J. A. Bull, R. A. Croft, O. A. Davis, R. Doran and K. F. Morgan, *Chem. Rev.*, 2016, **116**, 12150-12233.
33. K. B. Hansen, J. L. Leighton and E. N. Jacobsen, *J. Am. Chem. Soc.*, 1996, **118**, 10924-10925.
34. D. J. Darensbourg, A. I. Moncada, W. Choi and J. H. Reibenspies, *J. Am. Chem. Soc.*, 2008, **130**, 6523-6533.
35. D. J. Darensbourg and W.-C. Chung, *Polyhedron*, 2013, **58**, 139-143.
36. J. Chen, M. Zhong, L. Tao, L. Liu, S. Jayakumar, C. Li, H. Li and Q. Yang, *Green Chem.*, 2018, **20**, 903-911.
37. M. Cokoja, C. Bruckmeier, B. Rieger, W. A. Herrmann and F. E. Kühn, *Angew. Chem. Int. Ed.*, 2011, **50**, 8510-8537.
38. P. Bhanja, A. Modak and A. Bhaumik, *ChemCatChem*, 2019, **11**, 244-257.
39. M. Ding, R. W. Flaig, H.-L. Jiang and O. M. Yaghi, *Chem. Soc. Rev.*, 2019, **48**, 2783-2828.
40. D. Ma, J. Li, K. Liu, B. Li, C. Li and Z. Shi, *Green Chem.*, 2018, **20**, 5285-5291.
41. H. Koinuma and H. Hirai, *Makromol. Chem. Phys.*, 1977, **178**, 241-246.
42. H. Koinuma and H. Hirai, *Makromol. Chem. Phys.*, 1977, **178**, 1283-1294.
43. A. Baba, H. Meishou and H. Matsuda, *Makromol. Chem. Rapid Comm.*, 1984, **5**, 665-668.
44. A. Baba, H. Kashiwagi and H. Matsuda, *Tetrahedron Lett.* 1985, **26**, 1323-1324.
45. A. Baba, H. Kashiwagi and H. Matsuda, *Organometallics*, 1987, **6**, 137-140.
46. D. J. Darensbourg, A. Horn Jr and A. I. Moncada, *Green Chem.*, 2010, **12**, 1376-1379.
47. J. Rintjema, W. Guo, E. Martin, E. C. Escudero-Adán and A. W. Kleij, *Chem. Eur. J.*, 2015, **21**, 10754-10762.
48. C. J. Whiteoak, E. Martin, M. M. Belmonte, J. Benet-Buchholz and A. W. Kleij, *Adv. Synth. Catal.*, 2012, **354**, 469-476.
49. B. R. Buckley, A. P. Patel and K. G. Wijayantha, *Eur. J. Org. Chem.*, 2015, **2015**, 474-478.
50. M. Alves, B. Grignard, A. Boyaval, R. Méreau, J. De Winter, P. Gerbaux, C. Detrembleur, T. Tassaing and C. Jérôme, *ChemSusChem*, 2017, **10**, 1128-1138.
51. J. Huang, J. De Winter, A. P. Dove and O. Coulembier, *Green Chem.*, 2019, **21**, 472-477.
52. J. Huang, C. Jehanno, J. C. Worch, F. Ruipérez, H. Sardon, A. P. Dove and O. Coulembier, *ACS Catal.*, 2020, **10**, 5399-5404.
53. C.-J. Zhang, S.-Q. Wu, S. Boopathi, X.-H. Zhang, X. Hong, Y. Gnanou and X.-S. Feng, *ACS Sustain. Chem. Eng.*, 2020, **8**, 13056-13063.
54. H. R. Kricheldorf, R. Dunsing and A. S. I. Albet, *Makromol. Chem. Phys.*, 1987, **188**, 2453-2466.
55. H. R. Kricheldorf and J. Jossen, *J. Macromol. Sci. Chem.*, 1989, **26**, 631-644.

56. H. R. Kricheldorf and B. Weegen-Schulz, *Macromolecules*, 1993, **26**, 5991-5998.
57. J. Matsuo, K. Aoki, F. Sanda and T. Endo, *Macromolecules*, 1998, **31**, 4432-4438.
58. W. Hovestadt, A. J. Müller, H. Keul and H. Höcker, *Die Makromol. Chem. Rapid Comm.*, 1990, **11**, 271-278.
59. T. Takata, F. Sanda, T. Ariga, H. Nemoto and T. Endo, *Macromol. Rapid Commun.*, 1997, **18**, 461-469.
60. G. Rokicki, *Prog. Polym. Sci.*, 2000, **25**, 259-342.
61. H. R. Kricheldorf, J. Jossen and I. Kreiser-Saunders, *Makromol. Chem. Phys.*, 1991, **192**, 2391-2399.
62. W. Hovestadt, H. Keul and H. Höcker, *Polymer*, 1992, **33**, 1941-1948.
63. J. Yang, Y. Yu, Q. Li, Y. Li and A. Cao, *J. Polym. Sci., Part A: Polym. Chem.*, 2005, **43**, 373-384.
64. D. J. Darensbourg, P. Ganguly and D. Billodeaux, *Macromolecules*, 2005, **38**, 5406-5410.
65. D. J. Darensbourg, W. Choi, P. Ganguly and C. P. Richers, *Macromolecules*, 2006, **39**, 4374-4379.
66. M. Helou, O. Miserque, J. M. Brusson, J. F. Carpentier and S. M. Guillaume, *Chem. Eur. J.*, 2008, **14**, 8772-8775.
67. P. Dobrzynski, M. Pastusiak and M. Bero, *J. Polym. Sci., Part A: Polym. Chem.*, 2005, **43**, 1913-1922.
68. C. Li, Y. Wang, L. Zhou, H. Sun and Q. Shen, *J. Appl. Polym. Sci.*, 2006, **102**, 22-28.
69. I. Palard, M. Schappacher, B. Belloncle, A. Soum and S. M. Guillaume, *Chem. Eur. J.*, 2007, **13**, 1511-1521.
70. B. Zhao, C. Lu and Q. Shen, *J. Appl. Polym. Sci.*, 2007, **106**, 1383-1389.
71. D. Pospiech, H. Komber, D. Jehnichen, L. Häussler, K. Eckstein, H. Scheibner, A. Janke, H. R. Kricheldorf and O. Petermann, *Biomacromolecules*, 2005, **6**, 439-446.
72. J. Ling, Z. Shen and Q. Huang, *Macromolecules*, 2001, **34**, 7613-7616.
73. D. J. Darensbourg, P. Ganguly and W. Choi, *Inorg. Chem.*, 2006, **45**, 3831-3833.
74. D. J. Darensbourg and A. I. Moncada, *Inorg. Chem.*, 2008, **47**, 10000-10008.
75. P. Luger and J. Buschmann, *J. Am. Chem. Soc.*, 1984, **106**, 7118-7121.
76. D. J. Darensbourg and A. I. Moncada, *Macromolecules*, 2009, **42**, 4063-4070.
77. A. Sudo, Y. Morioka, E. Koizumi, F. Sanda and T. Endo, *Tetrahedron Lett.*, 2003, **44**, 7889-7891.
78. D. J. Darensbourg and A. I. Moncada, *Macromolecules*, 2010, **43**, 5996-6003.
79. M. North and R. Pasquale, *Angew. Chem. Int. Ed.*, 2009, **48**, 2946-2948.
80. C. Calabrese, L. F. Liotta, F. Giacalone, M. Gruttadauria and C. Aprile, *ChemCatChem*, 2019, **11**, 560-567.
81. M. Luo, X.-H. Zhang, B.-Y. Du, Q. Wang and Z.-Q. Fan, *Macromolecules*, 2013, **46**, 5899-5904.
82. M. Luo, X. H. Zhang and D. J. Darensbourg, *Acc. Chem. Res.*, 2016, **49**, 2209-2219.
83. M. Luo, Y. Li, Y.-Y. Zhang and X.-H. Zhang, *Polymer*, 2016, **82**, 406-431.

84. C.-J. Zhang and X.-H. Zhang, *Chin. J. Polym. Sci.*, 2019, 1-8.
85. K. Nakano, G. Tatsumi and K. Nozaki, *J. Am. Chem. Soc.*, 2007, **129**, 15116-15117.
86. S. Wu, M. Luo, D. J. Darensbourg and X. Zuo, *Macromolecules*, 2019, **52**, 8596-8603.
87. S. Wu, M. Luo, D. J. Darensbourg, D. Zeng, Y. Yao, X. Zuo, X. Hu and D. Tan, *ACS Sustain. Chem. Eng.*, 2020, **8**, 5693-5703.
88. D. Tan, X. Hu, Z. Cao, M. Luo and D. J. Darensbourg, *ACS Macro Lett.*, 2020, **9**, 866-871.
89. X.-H. Zhang, F. Liu, X.-K. Sun, S. Chen, B.-Y. Du, G.-R. Qi and K. M. Wan, *Macromolecules*, 2008, **41**, 1587-1590.
90. D. J. Darensbourg, J. R. Andreatta, M. J. Jungman and J. H. Reibenspies, *Dalton Trans.*, 2009, 8891-8899.
91. D. J. Darensbourg, S. J. Wilson and A. D. Yeung, *Macromolecules*, 2013, **46**, 8102-8110.
92. M. Luo, X.-H. Zhang and D. J. Darensbourg, *Macromolecules*, 2015, **48**, 5526-5532.
93. H.-L. Wu, J.-L. Yang, M. Luo, R.-Y. Wang, J.-T. Xu, B.-Y. Du, X.-H. Zhang and D. J. Darensbourg, *Macromolecules*, 2016, **49**, 8863-8868.
94. W.-M. Ren, T.-J. Yue, M.-R. Li, Z.-Q. Wan and X.-B. Lu, *Macromolecules*, 2017, **50**, 63-68.
95. X.-H. Cao, J.-L. Yang, H.-L. Wu, R.-Y. Wang, X.-H. Zhang and J.-T. Xu, *Polymer*, 2019, **165**, 112-123.